Astronomical Notes
Astronomische Nachrichten

A revisit to agglomerates of early-type Hipparcos stars

J.A. Caballero[1] and **L. Dinis**[2]

[1]   Dpto. de Astrofísica y Ciencias de la Atmósfera, Facultad de Ciencias Físicas, Universidad Complutense de Madrid, E-28040 Madrid, Spain
[2]   Grupo Interdisciplinar de Sistemas Complejos (GISC) and Dpto. de Física Atómica, Molecular y Nuclear, Universidad Complutense de Madrid, E-28040 Madrid, Spain

We study the spatial structure and sub-structure of regions rich in Hipparcos stars with blue $B_T - V_T$ colours. These regions, which comprise large stellar complexes, OB associations, and young open clusters, are tracers of on-going star formation in the Galaxy. The DBSCAN (Density-Based Spatial Clustering of Applications with Noise) data clustering algorithm is used to look for spatial overdensities of early-type stars. Once an overdensity, "agglomerate", is identified, we carry out a data and bibliographic compilation of their star member candidates. The actual membership in agglomerate of each early-type star is studied based on its heliocentric distance, proper motion, and previous spectro-photometric information. We identify 35 agglomerates of early-type Hipparcos stars. Most of them are associated to previously known clusters and OB associations. The previously unknown P Puppis agglomerate is subject of a dedicated study with Virtual Observatory tools. It is actually a new, nearby, young open cluster ($d \sim 470$ pc, age ~ 20 Ma) with a clear radial density gradient. We list P Puppis and other six agglomerates (including NGC 2451 A, vdBH 23, and Trumpler 10) as new sites for substellar searches because of their youth, closeness, and spatial density. We investigate in detail the sub-structure in the Orion, CMa-Pup and Pup-Vel OB complexes ("super-agglomerates"). We confirm or discover some stellar overdensities in the Orion complex, like the 25 Ori group, the Horsehead region (including the σ Orionis cluster), and the η Orionis agglomerate. Finally, we derive accurate parallactic distances to the Pleiades, NGC 2451 A, and IC 2391, describe several field early-type stars at $d < 200$ pc, and discuss the incompleteness of our search.

REPRINT

A revisit to agglomerates of early-type Hipparcos stars

J.A. Caballero[1,*] and **L. Dinis**[2]

[1] Dpto. de Astrofísica y Ciencias de la Atmósfera, Facultad de Ciencias Físicas, Universidad Complutense de Madrid, E-28040 Madrid, Spain

[2] Grupo Interdisciplinar de Sistemas Complejos (GISC) and Dpto. de Física Atómica, Molecular y Nuclear, Universidad Complutense de Madrid, E-28040 Madrid, Spain

We study the spatial structure and sub-structure of regions rich in Hipparcos stars with blue $B_T - V_T$ colours. These regions, which comprise large stellar complexes, OB associations, and young open clusters, are tracers of on-going star formation in the Galaxy. The DBSCAN (Density-Based Spatial Clustering of Applications with Noise) data clustering algorithm is used to look for spatial overdensities of early-type stars. Once an overdensity, "agglomerate", is identified, we carry out a data and bibliographic compilation of their star member candidates. The actual membership in agglomerate of each early-type star is studied based on its heliocentric distance, proper motion, and previous spectro-photometric information. We identify 35 agglomerates of early-type Hipparcos stars. Most of them are associated to previously known clusters and OB associations. The previously unknown P Puppis agglomerate is subject of a dedicated study with Virtual Observatory tools. It is actually a new, nearby, young open cluster ($d \sim 470$ pc, age ~ 20 Ma) with a clear radial density gradient. We list P Puppis and other six agglomerates (including NGC 2451 A, vdBH 23, and Trumpler 10) as new sites for substellar searches because of their youth, closeness, and spatial density. We investigate in detail the sub-structure in the Orion, CMa-Pup and Pup-Vel OB complexes ("super-agglomerates"). We confirm or discover some stellar overdensities in the Orion complex, like the 25 Ori group, the Horsehead region (including the σ Orionis cluster), and the η Orionis agglomerate. Finally, we derive accurate parallactic distances to the Pleiades, NGC 2451 A, and IC 2391, describe several field early-type stars at $d < 200$ pc, and discuss the incompleteness of our search.

1 Introduction

The works by Pannekoek (1929), Ambartsumian (1947) and Ruprecht (1981) were, according to de Zeeuw et al. (1999), among the most important ones for the understanding of the OB associations in the early pre-Hipparcos era. We also quote the comprehensive review by Blaauw (1964). OB associations are very young regions in the Galaxy containing high-mass O- and B-type stars. The ultraviolet radiation injected into the intra-association medium by these luminous blue stars play an important rôle on the subsequent low-mass star formation process. The study of OB associations is, therefore, necessary for answering critical questions in Astrophysics, like 'how does the fragmentation of a primordial molecular cloud take place', 'which is the shape of the initial mass function', 'how is the dynamical evolution at the first stages of a recently-born open cluster', 'where are the spiral arms of our Galaxy', or 'do early-type stars inhibit or facilitate the formation of substellar objects'.

After the *magnus opus* by de Zeeuw et al. (1999), who carried out a comprehensive census of the stellar content of nearby ($d < 1$ kpc) OB associations, based on Hipparcos positions, proper motions, and parallaxes, and prior

to launch of the European Space Agency (ESA) mission GAIA, very few "fresh" discoveries can be achieved on OB associations. The work by de Zeeuw et al. (1999) is not, however, the only search for star clusters and OB associations from the Hipparcos data: Platais, Kozhurina-Platais & van Leeuwen (1998) and Robichon et al. (1999) had previously done it (see also a posterior work by Baumgardt, Dettbarn & Wielen 2000).

The superior capabilities and results of the ESA astrometry mission Hipparcos (Perryman et al. 1997) have allowed astronomers to go on the characterization of the Galactic stellar populations in general, and of OB associations in particular. There have been other works with the Hipparcos catalogue aimed at studying particular regions containing early-type stars (Baumgardt 1998; de Bruijne 1999; Subramaniam & Bhatt 2000) or the Galactic structure attending to the spatial distribution of such stars (Comerón, Torra & Gómez 1998; Maíz-Apellániz 2001; Schröder et al. 2004). We all place our trust in the "fresh" discoveries on OB associations that will arise in the near future with the overwhelming GAIA dataset. It is expected, however, that the GAIA mission will be launched in the second half of 2011.

In the interim, we can still explore the OB associations with the Hipparcos catalogue and different aims, tools, and

* Corresponding author: caballero@astrax.fis.ucm.es

reductions of the raw data. On the one hand, in the current work, we have used the late re-reduction of the Hipparcos data by van Leeuwen (2007a), who has obtained improvements by up to a factor 4 in the astrometric accuracies for particular bright stars (see also details on the validation of the new Hipparcos reduction in van Leeuwen (2007b)). On the other hand, we have applied a novel (in Galactic astronomy) clustering analysis to part a dataset into subsets ("clusters" or "agglomerates"). Through *data clustering*, objects with a common distinguishing feature are classified into different groups. In our case, the common quality is just the spatial location of Hipparcos stars with blue colours (i.e. with early spectral types). That is, our aim is to study the structure (and super- and sub-structure) of Galactic OB associations, and derive some basic properties.

2 Analysis

2.1 Data clustering

2.1.1 Types of clustering

In short, data clustering is a common technique for statistical data analysis with the aim to classify elements into different groups or "clusters". It is widely used in some scientific disciplines, like computational biology (for gene finding or plant systematics), market research (for partitioning a population of consumers into market segments), or pattern recognition in machine learning (according to the clustering illusion, the natural human "see patterns where actually none exists"). There are several types of data clustering algorithms (and classifications, as well). The simplest categorization splits the clustering algorithms into hierarchical and partitional ones; hierarchical algorithms can be, in their turn, divisive or agglomerative. The similarity of two elements within a cluster is quantified with a distance measure, that is, in most of the cases, the Euclidean distance (there are also other distances, like the Manhattan, Mahalanobis, and Hamming ones). An agglomerative hierarchical clustering algorithm begins with each element as a separate cluster and, through comparison with other elements, progressively merges them into clusters. The single linkage clustering ("nearest neighbour") is a simple agglomerative method.

2.1.2 Clustering in astrophysics

Numerous astronomers and cosmologists have investigated hierarchical *extragalactic* clusterings (see a good example in White & Frenk 1991). Different algorithms to find groups, clusters, and superclusters of galaxies were early presented by, e.g., Turner & Gott (1976), Huchra & Geller (1982), Press & Davis (1982), Einasto et al. (1984), Barrow, Bhavsar & Sonoda (1985), Maddox et al. (1990), and Martínez et al. (1990). The used algorithms consisted in two-point angular correlation functions, minimal spanning trees, multifractal measures, percolations, an the well-tested

friends-of-friends (FoF) algorithm. More recent clustering analyses, particularly using data from the Sloan Digital Sky Survey and FoF-like algorithms, have been carried out by Merchán & Zandivarez (2002), Berlind et al. (2006), Weinmann et al. (2006), or Tago et al. (2008). Besides, Uchihori et al. (2000) looked for clusters of extremely high energy cosmic rays in the northern sky, which are in generally ascribed to extragalactic clusters.

At shorter distances, but still out of our Milky Way, there have been searches of OB associations using data clustering, mostly the Path Linkage Criterion, in the Magellanic System (Battinelli 1991; Bica & Schmitt 1995; Gouliermis et al. 2000), the Andromeda galaxy (Magnier et al. 1993; Battinelli, Efremov & Magnier 1996), and in other galaxies in the Local Group (Demers et al. 1995; Ivanov 1996; Pietrzyński et al. 2001). Although it is obvious to extrapolate the use of such automatic procedures to search for clusters in our own Galaxy, there have been very few works on this topic. First, Mel'nik & Efremov (1995) used the list of OB stars of Blaha & Humphreys (1989) as their input catalogue and the Path Linkage Criterion (that is a hierarchical agglomerative algorithm) to look for Galactic OB associations. Secondly, Reylé & Robin (2002) used the same method to search for (embedded) star clusters close to the Galactic plane with the Point Source Catalogue of the DENIS survey.

The spaghetti method used by de Zeeuw et al. (1999) and Hoogerwerf & Aguilar (1999) to identify OB associations and nearby moving groups, respectively, the 3-D and 2-D wavelet analysis carried out by Chereul, Crézé & Bienaymé (1998, 1999) and Skuljan, Heranshaw & Cottrell (1999), and other maximum likelihood approaches (Chen et al. 1997; Asiain et al. 1999) can also be considered as uncommon examples of data clustering in the Galaxy. However, all those methods require, in general, a complex mathematical apparatus and information on the star proper motion and, sometimes, age. At the long heliocentric distances where most of the OB associations are found ($d \geq 200$ pc), their stellar populations are difficult no disentangle from the background solely based on proper motions, that are typically very low ($\mu \leq 10$ mas a^{-1}). The data clustering algorithm that we use in this paper resembles the FoF *extragalactic* algorithm, that is much easier to implement, and only requires as input the 2-D spatial coordinates (α, δ) of the stars. Uncertainties in the parallax determination of the farthest Hipparcos stars may prevent the use of a 3-D FoF-like algorithm (this task will be performed in the future with GAIA data).

2.1.3 Our clustering algorithm

In this section, we will use the term "cluster" to define the groupings of stars obtained by the algorithm, to use the standard nomenclature in data clustering. However, in the following sections, we will use the term "agglomerate" for the different groupings of stars that the algorithm returns. This choice is to avoid confusion with the term "(star) cluster".
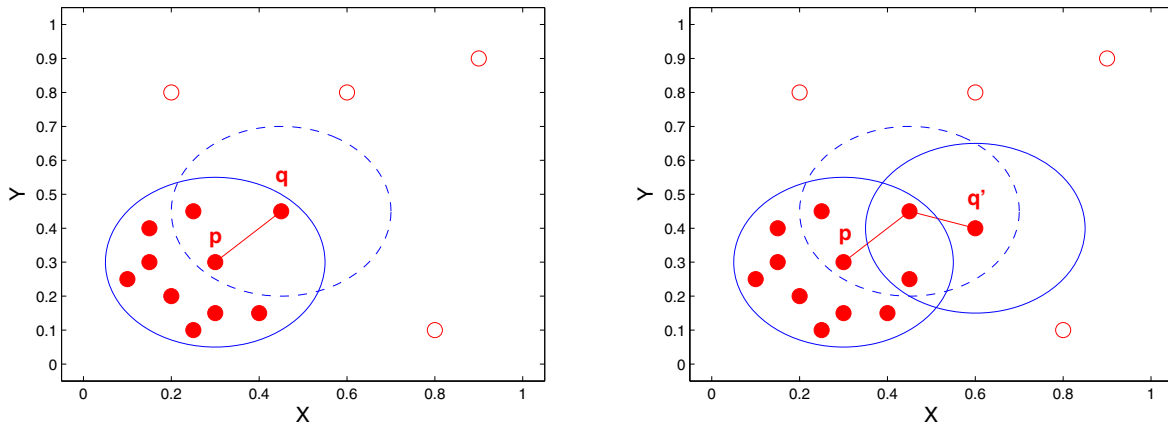
Fig. 1 (online colour at: www.an-journal.org) A core point p and a border point q (*left*) and a point q' density-reachable from p through an intermediate (core) point (*right*) for $N_{\mathrm{MinPts}} = 4$ and $R_\epsilon = 0.25$ in arbitrary units. Filled symbols represent cluster points.

Other expressions that we must avoid using are "(moving) group" and "(OB) association". Obviously, we expect the clustering algorithm to provide agglomerates of early-type stars that ultimately belong to a star cluster, a moving group, or an OB association, but their membership can only be confirmed after a follow-up of the individual stars.

Among the available algorithms for data clustering, we chose DBSCAN (Density-Based Spatial Clustering of Applications with Noise) for its ability to recognise clusters of arbitrary shape in a database with "noise", that is, a number of points that do not necessarily belong to any cluster. Recalling Sect. 2.1.1, DBSCAN is an Euclidean agglomerative hierarchical clustering algorithm. We will just outline here the fundamental aspects of density-based clustering and describe briefly the algorithm. A more detailed description of DBSCAN, including a pseudo-code, can be found in Ester et al. (1996).

The notion of cluster in DBSCAN resides in the fact that the density inside a cluster is considerably higher than outside it, in the noise. This situation clearly resembles our problem, that consists in picking out densely packed groups of stars in an apparently random 2-D spatial distribution. To ensure that the clusters recognised by the algorithm are sufficiently dense, one may naïvely require that there are at least a minimum number of points (N_{MinPts}) in a ball of radius R_ϵ around every point p in a cluster. A ball of radius R_ϵ centred on p is usually termed the neighbourhood of p. There are, however, two kinds of points in a cluster: points well inside the cluster, or *core points*, and points in the border, or *border points*. A border point has less cluster points inside its neighbourhood than a core point, as shown in left window of Fig. 1. To include all points in a cluster, N_{MinPts} should be set to a low value, what makes difficult for the algorithm to distinguish clusters from noise. To solve this difficulty, DBSCAN requires that for every point q in the cluster there is another point p in the cluster so that q is inside the neighbourhood of p, and the neighbourhood of p contains at least N_{MinPts} points (i.e., p is a core point). If q

is in the neighbourhood of a core point but is not a core point itself then q is a border point. The following definition is central to turning this idea into an useful algorithm: a point q is said *density-reachable* from p if there is a chain of points $p = p_1 \rightarrow p_2 \rightarrow p_3 \ldots p_n = q$ such that p_{i+1} is in the neighbourhood of p_i, and the neighbourhood of p_i contains at least N_{MinPts} points. A sensible definition of a cluster is, then, *the set of all points that are density-reachable from a core point*, which includes all the core points as well as all the possible border points.

In short, DBSCAN starts from the first point q in the database and finds all points in its neighbourhood. If q is not a core point, DBSCAN tentatively marks q as noise and proceeds to the next point p. If p is a core point, all the density-reachable points from p are found and marked as belonging to the same cluster. DBSCAN then proceeds to the next unclassified point in the database, repeating the procedure until all the points are marked either as noise or belonging to a cluster (i.e. an agglomerate).

2.2 Input catalogue

Before looking for possible agglomerates of early-type Hipparcos stars, we had to build the input dataset for our DBSCAN algorithm. By "early-type" we mean "with approximate spectral types O and B". Slightly more than 97 % of the stars in the original Hipparcos catalogue ($N_0 = 118\,218$) have no blanks in the parallax, proper motions, and $B_\mathrm{T} V_\mathrm{T}$ photometry fields, simultaneously ($N_1 = 114\,820$). Among them, we selected all the sources with Tycho[1] colours $B_\mathrm{T} - V_\mathrm{T} < -0.05$ mag ($N_2 = 4\,142$). No additional restriction was imposed. These objects are the input for the clustering analysis described below. Figure 2 illustrates our simple colour selection procedure.

---

[1] For an easier analysis, we have used the Tycho-1 magnitudes (Perryman et al. 1997) instead of the slightly more precise Tycho-2 ones (Høg et al. 2000).
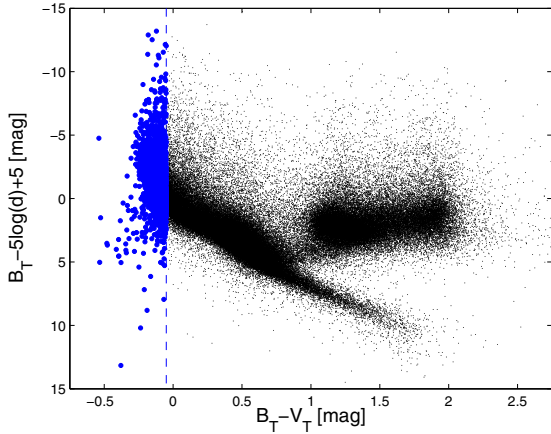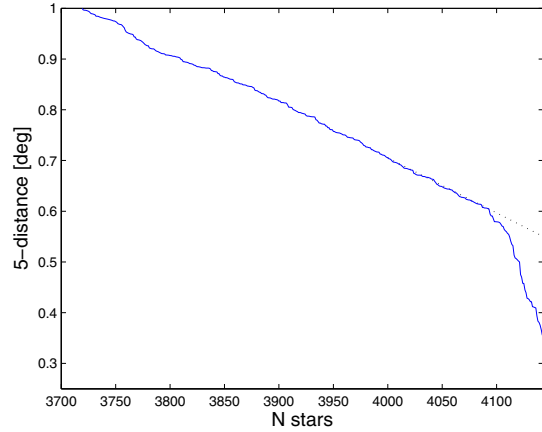
Fig. 2 (online colour at: www.an-journal.org) $B_{\rm T} - 5 \log d + 5$ vs. $B_{\rm T} - V_{\rm T}$ diagram of the $N_1 = 114\,820$ Hipparcos stars with no blanks in the parallax, proper motions, and $B_{\rm T} V_{\rm T}$ photometry fields. It is roughly a colour-absolute magnitude ($M_{B_{\rm T}}$) diagram, except for the interstellar extinction factor in the $B_{\rm T}$ band, that is not taken into account. The $N_2 = 4\,142$ selected stars with Tycho colours $B_{\rm T} - V_{\rm T} < -0.05$ mag are located to the left of the dashed vertical line.

Except for relatively high-amplitude variability, large photometric uncertainty (due to star faintness or partially resolved multiplicity), the inaccurate Johnson-Tycho systems transformation at blue colours, and the existence of white dwarfs and bright He-B subdwarfs below the main sequence, the great majority of the selected sources are O- and B-type dwarfs, giants and supergiants. The input dataset also contains a few stars with early-A spectral types; in many cases, it is due to an incorrect spectral type determination rather than to errors in the colours. Of the 11 objects with Tycho colours $B_{\rm T} - V_{\rm T} < -0.05$ mag and absolute magnitudes $M_{B_{\rm T}} \approx B_{\rm T} - 5 \log d + 5 > 5$ mag, six are white dwarfs (including the intrinsically very faint, nearby, DC-type white dwarf GJ 440), three are B9-type dwarfs and giants with incorrect parallax determinations, one is a subdwarf (HD 188112), and one is an incorrectly identified star (BD+05 1825; see Sect. 4.7).

2.3 Parameter selection

To choose the proper parameters for the analysis, we started by setting the minimum number of bright blue stars in the cluster to a reasonable value, $N_{\rm MinPts} = 6$. Decreasing this limit would lead us to consider an unmanageable amount of agglomerates, many of which would actually be spurious groupings.

To obtain the order of magnitude of the radius R_ϵ, we used the following heuristic argument: first, we computed the ($N_{\rm MinPts} - 1$)-distance function, mapping every point (star) in our input catalogue with the angular distance to its fifth nearest neighbour ("5-distance"). We sorted the 5-distance vector by ordering all its elements in decreasing order of their value. Figure 3 shows a detail of the sorted

Fig. 3 (online colour at: www.an-journal.org) Sorted 5-distance plot of the bright blue stars with the shortest 5th-distances in the input catalogue. A difference in the slope is apparent for values above and below 0.6 deg (the dotted line extrapolates the 5-distance for $R_\epsilon < 0.6$ deg).

5-distance, that carries information about the distribution of distances in the database (Ester et al. 1996). By setting R_ϵ to some fixed value, all the points (stars) with 5-distance $\leq R_\epsilon$ will be core points. In the figure, we see that there is a critical value at $R_\epsilon \sim 0.6$ deg that marks a change in behaviour. The number of points assigned to an agglomerate grows rapidly with increasing R_ϵ below 0.6 deg, indicating that larger increases of R_ϵ above that value are needed to see a significant change in the number of detected agglomerates. Once above the critical value, the results will not vary dramatically. From this, we can deduce that a value of $R_\epsilon \geq 0.6$ deg should be used.

On the other hand, the DBSCAN algorithm detects aggregates with density of approximately $N_{\rm MinPts}/(\pi R_\epsilon^2)$ or higher. We used a very well known cluster, the Pleiades, as a template for computing an order of magnitude of the densities that we expect to find in our input catalogue. From the equality between densities, the neighbourhood radius is $R_\epsilon = R_{\rm Ple}(N_{\rm MinPts}/N_{\rm Ple})^{1/2}$. We have identified $N_{\rm Ple} = 10$ classical Pleiads as Hipparcos stars with colours $B_{\rm T} - V_{\rm T} < -0.05$ mag. All of them are contained within a 1 deg-radius circle centred on Alcyone (i.e. $R_{\rm Ple} \sim 1.0$ deg), which makes $R_\epsilon \sim 0.8$ deg. Considering this, we increased R_ϵ from 0.6 to 0.8 deg in order to decrease the threshold density of the algorithm below the density of bright blue stars in the Pleiades. A discussion on the effect of the parameterization on the results (e.g. $R_\epsilon = 0.6, 0.8, 1.0$ deg) is in Sect. 4.6.

3 Results

Using the parameters $N_{\rm MinPts} = 6$, $R_\epsilon = 0.8$ deg, our DB-SCAN clustering algorithm has identified 406 Hipparcos stars with $B_{\rm T} - V_{\rm T} < -0.05$ mag distributed among 35

Table 1   Agglomerates of early-type Hipparcos stars.

Agglomerate	Reference Star	l (deg)	b (deg)	Super-Agglomerate	Cluster/Association/ Complex/Region	$N_\star$	Possible Contaminant(s)
Escorial 1	Alcyone	166.7	–43.1	...	Pleiades	10	...
Escorial 2	V1360 Ori	196.1	–22.5	Orion	...	6	(Spurious agglomerate)
Escorial 3	25 Ori	201.0	–18.3	Orion	Ori OB1 a, 25 Orionis	23	HD 35716, HD 35926 AB
Escorial 4	η Ori	204.9	–20.4	Orion	Ori OB1 a, η Orionis	9	HD 35957
Escorial 5	θ^{01} Ori C	209.0	–19.4	Orion	Ori OB1 d, Orion Nebula	23	...
Escorial 6	Alnilam	205.2	–17.2	Orion	Ori OB1 b, Collinder 70	23	...
Escorial 7	σ Ori	206.8	–17.4	Orion	Ori OB1 b, σ Orionis	7	...
Escorial 8	10 Mon	214.5	–7.4	...	NGC 2232	9	HD 45153, HD 45975
Escorial 9	S Mon AB	202.9	+2.2	...	NGC 2264, Christmas Tree	6	...
Escorial 10	EZ CMa	234.8	–10.1	CMa-Pup	Collinder 121	21	...
Escorial 11	HH CMa	233.5	–8.7	CMa-Pup	Collinder 121	19	...
Escorial 12	24 CMa	235.6	–8.2	CMa-Pup	Collinder 121	32	HD 53123
Escorial 13	FV CMa	236.0	–7.3	CMa-Pup	Collinder 121	7	...
Escorial 14	HD 55019	240.7	–9.0	CMa-Pup	Collinder 121	6	...
Escorial 15	27 CMa AB	239.0	–7.1	CMa-Pup	Collinder 121	15	ω CMa
Escorial 16	HD 55879	224.7	+0.4	...	NGC 2353	9	...
Escorial 17	HD 56342	243.0	–8.8	CMa-Pup	Collinder 132	11	HD 56342
Escorial 18	τ CMa AB	238.2	–5.5	CMa-Pup	Collinder 121, NGC 2362	16	...
Escorial 19	NO CMa	244.9	–7.9	CMa-Pup	Collinder 140	10	HD 58285
Escorial 20	HD 59138	241.0	–4.7	CMa-Pup	Collinder 121	9	HD 59364
Escorial 21	BD–14 2020 AB	231.0	+3.1	...	M 47	6	...
Escorial 22	HD 61071	240.4	–2.2	CMa-Pup	Collinder 121	6	m Pup A(C)B (?)
Escorial 23	HD 61987	243.2	–2.6	CMa-Pup	(Collinder 121)	8	k^{01} Pup AB, HD 61687 AB
Escorial 24	c Pup	252.4	–6.7	Pup-Vel	NGC 2451 A, NGC 2451 B	14	V468 Pup
Escorial 25	QS Pup	260.6	–10.4	Pup-Vel	Vel OB2, P Puppis	10	HD 63007
Escorial 26	γ Vel	262.8	–7.7	Pup-Vel	Vel OB2, NGC 2547	21	HD 67704, HD 67847, HD 68657
Escorial 27	OS Pup	254.0	–1.0	Pup-Vel	vdBH 23, Pup OB3	11	HD 68450
Escorial 28	NO Vel AB	262.9	–6.9	Pup-Vel	Vel OB2	6	...
Escorial 29	IT Vel	263.4	–6.3	Pup-Vel	Vel OB2	10	HD 70251
Escorial 30	HD 72997	262.9	–2.6	Pup-Vel	vdBH 34, Pismis 4, Vel OB2	6	...
Escorial 31	o Vel	270.3	–6.8	Pup-Vel	IC 2391	7	...
Escorial 32	HX Vel	266.6	–3.6	Pup-Vel	IC 2395	6	HD 74273
Escorial 33	HD 75387	262.8	+0.7	Pup-Vel	Trumpler 10	10	...
Escorial 34	HD 194670	78.1	+1.1	...	"HIP 98321"	8	...
Escorial 35	8 Lac AB	96.4	–16.1	...	Lac OB1	6	...

agglomerates. These agglomerates are summarized in Table 1. We follow the nomenclature 'Escorial'[2] plus a running number to designate the agglomerates. The number of stars per agglomerate varies between $N_\star = 6$ (the minimum number) and 32. The spatial location of all the Hipparcos stars and those with blue colours are shown in top and middle windows in Fig. 4.

Eight of the agglomerates are "isolated", while the remaining ones seem to be associated in "super-agglomerates" (i.e. agglomerates of agglomerates). Although we have not carried out a quantitative study to distinguish super-agglomerates, they naturally arise from a simple visual inspection of the results. Besides, the existence of these super-agglomerates is endorsed by lots of previous works. One of our super-agglomerates is linked to the very famous Orion complex. The other large agglomeration of agglomerates, that occupies an extended area in the Canis Majoris-Puppis-Vela region (CMa-Pup-Vel; Kaltcheva & Hilditch 2000), has been splitted into two differentiated super-agglomerates for simplicity. We have named them Canis Majoris-Puppis (CMa-Pup) and Puppis-Vela (Pup-Vel). The ass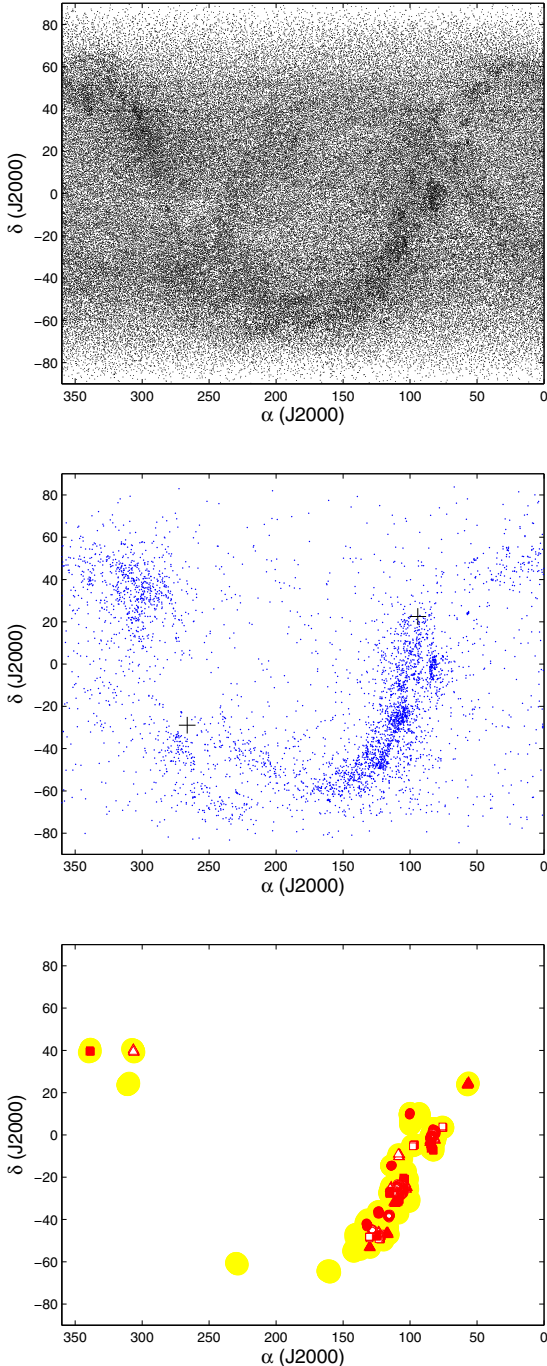ociations Ori OB1 (Orion), Collinder 121, CMa OB1, Pup OB1, and Vel OB2 (in CMa-Pup-Vel) belong to the local spiral arm of the Galaxy (Humphreys 1978). Many of the known clusters and associations were also tabulated by Piskunov et al. (2006) as member candidates of the open cluster complex OCC 1 (which is apparently a signature of Gould's Belt).

The super-agglomerates, agglomerates and respective stellar components are described next and listed in detail in Table A1. Heliocentric distances in parenthesis are from the original Hipparcos reduction (Perryman et al. 1997), with lower error bars (only in these particular cases) than in van Leeuwen (2007a). Possible fore- and background blue contaminants or interlopers are also discussed. Images of the agglomerates can be found in the Appendix in the electronic version of the journal (Figs. A1 to A12).

3.1   Isolated agglomerates

Our clustering algorithm has identified seven agglomerates that are not ascribed to the Orion, CMa-Pup, or Pup-Vel super-agglomerates. Many of them are associated to known young open clusters or star-forming regions. Furthermore, a few of them, like the Pleiades (the template cluster for our R_ϵ choice), NGC 2264, or IC 2391, are among the best studied open clusters. Four of the seven agglomerates, in the Monoceros-Puppis region, are shown in Fig 5.

---

[2] El Escorial, a Madritian municipality famous for its nearby Monasterio de El Escorial (a UNESCO World Heritage Site), is the hometown of both JAC and LD.

3.1.1 Escorial 1 (Pleiades)

The Pleiades (M 45, Melotte 22, the Seven Sisters) is the open cluster *par excellence*. Known since antiquity, it is the most obvious cluster to the naked eye. Given its short heliocentric distance, the Pleiades stars have been widely used as calibrators for evolutionary models and as star candles (Johnson & Mitchell 1958; Vandenberg & Bridges 1984; Soderblom et al. 1993; Stauffer et al. 1994). The first brown dwarf, Teide 1, was discovered in this cluster (Rebolo, Zapatero Osorio & Martín 1995).

The ten stars in the Escorial 1 agglomerate, with B6–8 spectral types and different classes of luminosity (III, IV, and V; see Table A1), have magnitudes, proper motions, and parallaxes consistent with membership in the Pleiades cluster. Although we have identified the ten Hipparcos stars in the region with the bluest $B_T - V_T$ colours as members of the agglomerate, they do not match the classical list of the brightest cluster stars. Absent classical Pleiads are Asterope and Celaeno, with $B_T - V_T \geq -0.05$ mag, while other identified, blue, not-so-bright Pleiads are 18 Tau and HD 23753. No contaminants have been identified. See Sect. 4.4.1 for a discussion on the Pleiades heliocentric distance.

3.1.2 Escorial 8 (NGC 2232)

The NGC 2232 is a poorly known, young, open cluster in Monoceros. Its brightest members is the β Cep-type variable star 10 Mon (B2V). Clariá (1972) carried out the first detailed photometric study of the cluster, although Herschel (1864), Dreyer (1888), and Collinder (1931) had previously catalogued it. There have been few late spectroscopic, photoelectric, and astrometric analyses (Levato & Malaroda 1974; Pastoriza & Ropke 1983; Jenkner & Maitzen 1987). More recently, Lyra et al. (2006) determined nuclear and contraction ages in the narrow interval 25–32 Ma, and an heliocentric distance of $d = 320 \pm 30$ pc. To finish the short historical review, Dias et al. (2002) tabulated an angular diameter of about 1 deg.

Our list of nine Hipparcos stars in the Escorial 8 agglomerate roughly matches those of NGC 2232 member candidates by Robichon et al. (1999) and Baumgardt et al. (2000), as well as the brightest stars listed by Clariá (1972). The slight differences consist in the nature of a couple of possible interlopers. We have identified two contaminants, HD 45153 and HD 45975. They are two B8–9V-type stars at $d \sim 200$ pc and proper motions inconsistent with membership in cluster. The NGC 2232 cluster seems to be located, from our Hipparcos data, at 330 ± 50 pc. This distance agrees very well with the value derived by Lyra et al. (2006) from main-sequence fitting.

3.1.3 Escorial 9 (NGC 2264)

The NGC 2264 cluster in the Mon OB1 association contains four structures that show clear evidence of extreme

Fig. 4 (online colour at: www.an-journal.org) Spatial distribution of early-type Hipparcos stars in agglomerates. *Top*: all the $N_1 = 114\,820$ Hipparcos stars with no blanks in the parallax, proper motions, and $B_T V_T$ photometry fields. *Middle*: $N_2 = 4\,142$ selected stars with Tycho colours $B_T - V_T < -0.05$ mag. Crosses mark the Galactic centre (left/southeast) and anticentre (right/northwest). The plane of the Galactic disc is clearly discernible. The void of blue stars to the north of the Galactic centre is the Ophiuchus-Serpens region. Most of the apparent overdensities are discussed next. *Bottom*: blue Hipparcos stars in agglomerates with DBSCAN parameters $N_{MinPts} = 6$ and $R_\epsilon = 0.8$ (small red different symbols), and $N_{MinPts} = 6$ and and 1.0 deg (large yellow filled circles). Escorial 34 (open triangles) and 35 (filled squares) are the easternmost agglomerates.

Fig. 5 (online colour at: www.an-journal.org) Spatial location of the stars of the agglomerates Escorial 8 (NGC 2232) and Escorial 9 (NGC 2264) in Monoceros, and Escorial 16 and Escorial 21 (M 17) in Puppis, in (red) different symbols (from west to east). Other early-type Hipparcos stars are marked with tiny (blue) dots. Note the overdensities corresponding to the Orion complex (at $\alpha \sim 80$–85 deg, $\delta \sim \pm 5$ deg) and the north of the CMa-Pup agglomerate (to the south of the plot).

youth (age ~ 3 Ma) and on-going star formation: the Christmas Tree Cluster, the Fox Fur Nebula, the Snowflake Cluster, and the Cone Nebula. Although the four structures have been considered as a single entity (precisely called NGC 2264), a purist would contradict this statement: the stellar cluster that is actually identified in the optical is the Christmas Tree Cluster, including the bright pre-main sequence star S Mon AB (O7Ve). The latter star illuminates the nearby Fox Fur Nebula and the more distant Cone Nebula (the tip of which is just a few arcmin away from the pre-main sequence giant HD 47887, B2III). The nicknamed Snowflake Cluster is a dense collection of embedded, low-mass stars detected at mid-infrared and submillimetric wavelengths, adjacent to the NGC 2264 IRS2 source (Young et al. 2006), and at half distance between S Mon AB and the Cone Nebula. The "NGC 2264" cluster as a whole has been widely used to test stellar formation scenarios, measure frequencies of discs, and study T Tau stars and outflows (e.g. Walker 1956; Strom et al. 1972; Rebull et al. 2002; Lamm et al. 2004; Dahm & Simon 2005).

From our clustering analysis, only six blue Hipparcos stars (the minimum number) belong to the Escorial 9 agglomerate, being S Mon AB the brightest one. Of the remaining five stars, three are relatively well known pre-main-sequence stars, and two are of unknown nature. The latter stars, HD 47754 (B9V) and HD 47662 (B7V, a low-amplitude photometric variable – Koen & Eyer 2002), are located quite to the north of the compact H II region on the centre of NGC 2264. Their area is still rich in emission-line and variable stars, as well as Herbig-Haro objects, so the two early-type stars may also belong to the young star-forming region.

The close separation between the components of S Mon AB ($\rho = 2.909 \pm 0.013$ arcsec, $\Delta H_p = 3.33 \pm 0.06$) may have affected the Hipparcos parallactic distance determination of the system, which is clearly incorrect ($d = 280 \pm 40$ pc; S Mon AB would be located at a significantly shorter heliocentric distance than the other members of NGC 2264, at about 600–800 pc).

3.1.4 Escorial 16

The Escorial 16 agglomerate contains nine stars. Two of them, HD 55879 and HD 55755, were classified as members of the moderately young NGC 2353 open cluster by Hoag et al. (1961). This cluster is quite compact (about 15 arcmin) and located near the edge of the very young CMa OB1 association (age ~ 3 Ma – see an excellent review on the association in de Zeeuw et al. 1999). The most comprehensive study and review of NGC 2353 to date was carried out by Fitzgerald, Harris & Reed (1990). According to them, the cluster is at the same distance as CMa OB1 ($d = 1200 \pm 80$ pc), but is several times older (age ~ 76 Ma). They concluded, therefore, that NGC 2353 and CMa OB1 are unrelated, and that the brightest star in the area, HD 55879 (an early B-/late O-type giant), does not belong to the cluster, but to CMa OB1. HD 55755 would remain as the only Hipparcos star member of NGC 2353. These results are not conclusive, because Hoag et al. (1961) assumed a younger age of NGC 2353, rather similar to the age CMa OB1.

There are other seven stars at up ~ 1.3 deg to the NGC 2353 centre that belong to the Escorial 16 agglomerate. Only one of them is remarkable: HD 55135. It was one of the first emission-line, B-type (Be) stars to be discovered (Merrill, Humason & Burwell 1925). Its strong Hα emission might indicate that it is also a few megayears old (unless Be stars are "the remnants of case B mass transfer in intermediate-mass close binaries"; Pols et al. 1991), and then HD 55135 could even be younger than NGC 2353. Of the remaining stars, HD 55117 had an Hipparcos solution flagged as unreliable (we have taken the values for its distance and proper motions from Falin & Mignard (1999)). The other four stars have been only glanced by Clariá (1974) or have no references at all.

Obviously, further spectro-photometric analyses are needed to disentangle between the populations of NGC 2353 and CMa OB1, and to ascertain the actual nature of the Escorial 16 agglomerate. It might be a random overdensity in the disperse CMa OB1 association.

3.1.5 Escorial 21 (M 47)

The agglomerate Escorial 21 is associated to the young open cluster M 47 (NGC 2422 – Zug 1933; Smyth & Nandy 1962; Shobbrook 1984; Nissen 1988; Barbera et al. 2002; Prisinzano et al. 2003). It is a ~ 100 Ma-old cluster at ~ 470 pc (Rojo Arellano, Peña & González 1997), with a

minimum diameter of half a degree and a very low reddening. It has been repeatedly considered as a (more distant) Pleiades twin.

Our six stars in the Escorial 21 agglomerate are among the brightest stars of the cluster. There are only two missing bright stellar systems: the (at least) quintuple system BD–14 2020 (the Hipparcos reduction probably failed because of the intense brightness of, and closeness between, the A and B components; $V_{A,B} \sim 6.5$–7.0 mag, $\rho \approx 7.2$ arcsec) and the spectroscopic binary KQ Lup AB (an A4Ia supergiant with a quite red $B_T - V_T$ colour). Our list of M 47 member stars basically coincides with that of Robichon et al. (1999). The weight-averaged parallactic distance from the re-reduced Hipparcos stars of our six early-type stars is $d = 450 \pm 100$ pc, that also match with previous estimates.

3.1.6 Escorial 34 and 35

The 14 stars in the Escorial 34 ($N_\star = 8$) and 35 ($N_\star = 6$) agglomerates are located far away from the previous isolated clusters and from the Orion, CMa-Pup, and Pup-Vel superagglomerates. They lie in the Cygnus-Lacerta region of the Galactic plane, roughly equidistant from the North America (NGC 7000) and Cocoon (IC 5146) nebulae.

The stars of the Escorial 34 agglomerate are embedded in the γ Cyg H II nebula (IC 1318), whose centre roughly coincides with the supergiant Sadr (F8Iab, $V \approx 2$ mag – Sadr is in the centre of Cygnus' cross). They are close to the M 29 open cluster, but there is no indication for their membership in there. Dolidze (1961) reported a star cluster near Sadr, Dolidze 10, but we have not been able to identify it. The eight stars in the agglomerate are poorly known: there is some kind of membership information only for the four easternmost ones. The four stars (with spectral types B8 to A0 – see Table A1) were classified by Platais et al. (1998) as members of the crowded "HIP 98321" association, that occupies an extended area around the star HIP 98321 (HD 189433) and covers parts of Cepheus, Cygnus, Lyra, and Vulpecula. This association extends up to 12 deg and is located at about 300 pc from the Sun (Madsen, Dravins & Lindegren 2002). Precisely, the four "HIP 98321" stars have the shortest heliocentric distances in the Escorial 34 agglomerate ($d \sim 260$–370 pc). HD 194885, with estimated spectral type A0 and an heliocentric distance of 260 ± 20 pc, may be an interloper of the "HIP 98321" association. The remaining four (westernmost) stars in the agglomerate, with slightly different proper motions and poorly determined Hipparcos distances, are probably background early-type stars of the Orion-Cygnus spiral arm (see, e.g., Comerón et al. (1993) for a discussion on the good visibility of the stars of this arm from the Sun position). As a result, the Escorial 34 agglomerate does not seem to be a single physical grouping of stars.

The six stars in the Escorial 35 agglomerate are members of the Lac OB1 association (Blaauw & Morgan 1953; Hardie & Seyfert 1959; Guetter 1976). The peculiar binary

HD 213918 AB is the only Hipparcos star of the agglomerate that is not in the list of Lac OB1 members by de Zeeuw et al. (1999), but several other works support their membership in the association (Crawford 1961; Adelman 1968; Levato & Abt 1976). It is obvious that the Escorial 35 agglomerate does not represent the whole Lac OB1 association, but a quite small fraction (de Zeeuw et al. (1999) tabulated 96 Hipparcos members of the association). Previous claims of sub-structure within Lac OB1 have been reported (see Lesh (1969), de Zeeuw et al. (1999), and references therein for a discussion on the Lac OB1 "a" and "b" subgroups). As a support for our identification, Kharchenko et al. (2005) listed four of our Hipparcos stars (actually six stars in three multiple systems, including the resolved binary 8 Lac A and B) as members of the new Galactic open cluster [KPR2005] 122 (ASCC 122). Additional studies are needed to confirm if this overdensity of early-type stars within Lac OB1 is a physical grouping or not.

3.2 The Orion super-agglomerate

Apart from Cep OB1, that was not so well investigated at that moment, the Ori OB1 complex was the most massive OB association in the 1 kpc sphere centred on the Sun in the classical review by Blaauw (1964). It was, besides, more compact than the other massive Scorpius-Centaurus and Lac OB1 complexes. The total mass and largest overall projected diameter estimated by him for the Ori OB1 complex, at about $7600\,\mathrm{M}_\odot$ and 100 pc, roughly match current determinations. The currently accepted division of Ori OB1 into four subgroups was also presented by Blaauw (1964). He proposed the following sub-associations:

– Ori OB1a: north and west of the Orion Belt,
– Ori OB1b: the Orion Belt itself,
– Ori OB1c: south and east of the Orion Belt, except the Orion Sword,
– Ori OB1d: in and close to the Orion Sword.

Warren & Hesser (1977) splitted, in its turn, the Ori OB1b subgroup into three sub-subgroups (b1, b2, and b3), and the Ori OB1c subgroup into five sub-subgroups (c, c1, c2, c3, and c4). The nine groupings are supposed to have different ages and heliocentric distances, in the intervals 1–10 Ma and 350–500 pc, respectively, being Ori OB1d (including the Orion Nebula Cluster and the Trapezium) the youngest one. Further classical reviews on the Orion molecular cloud and star-forming region, emphasizing on its importance in modern astronomy, can be found at Genzel & Stutzki (1989) and Brown, de Geus & de Zeeuw (1994).

Our DBSCAN algorithm has identified six agglomerates in the region 05 00 $\leq \alpha \leq$ 05 40, $-8 \leq \delta \leq +4$, quite close to the Solar antapex. Any blue star with low proper motion in this area is capable of belonging to the Ori OB1 complex. We consider that all but one of these agglomerations are actual members of the complex. Since they do not exactly correspond to the classical grouping in the cluster, we will follow the "Escorial" designation. See Sect. 4.3 for a discussion on the sub-structure of the Orion super-agglomerate.
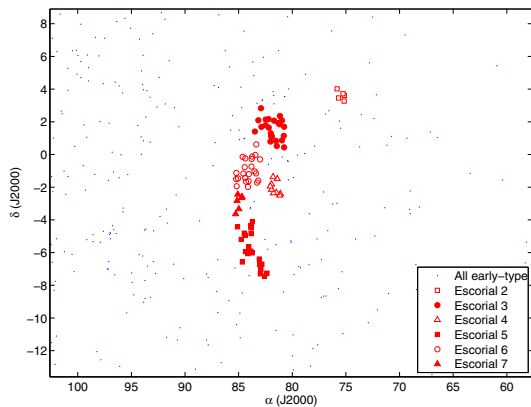
Fig. 6 (online colour at: www.an-journal.org) Same as Fig. 5, but for the agglomerates Escorial 2–7 in the Orion super-agglomerate.

3.2.1 Escorial 2

This agglomerate of only six stars, with B8–9V spectral types, is in a distinct location with respect to the other five agglomerates. Far from presenting it as a new subgroup in the Ori OB1 complex, we consider Escorial 2 a spurious agglomeration. This hypothesis is supported, apart from the different location, by: (i) the low number of stars in the agglomerate (the minimum N_{MinPts}), (ii) their relatively late spectral types, (iii) the heliocentric distances shorter than 300 pc of at least two (possibly four) stars, and (iv) the presence of two of the stars in a close binary (HD 32039, HD 32040; if they were a single star, then $N_\star = 5 < N_{\mathrm{MinPts}}$ and DBSCAN would have not recognize it as an agglomerate).

3.2.2 Escorial 3 (25 Orionis)

The 23 stars in the Escorial 3 agglomerate lay on the northern part of the Ori OB1a subgroup, surrounding the bright B1Vpe star 25 Ori (also known as ψ^{01} Ori)[3]. In spite of the large amount of stars in the agglomerate, the group was not identified until very recently, when Briceño et al. (2005) and Kharchenko et al. (2005) discovered what they called the "25 Ori group" and the "ASCC 16 cluster" ([KPR2005] 16), respectively. Many of the stars in our agglomerate, including 25 Ori itself, have been catalogued in those works, which supports a correct identification. While for Briceño et al. (2005) the Escorial 3 agglomerate stood out as a concentration of T Tau stars in the Ori OB1a sub-association, Kharchenko et al. (2005) found it based on parallaxes, proper motions, and $B_{\mathrm{T}}V_{\mathrm{T}}$ photometry for Hipparcos and Tycho-2 stars. The confirmation of Escorial 3 having dis-

tinct kinematics (in V_{r}) and age (7–10 Ma) in Ori OB1a was presented by Briceño et al. (2007).

Not all the 23 stars belong to the young agglomerate. In Table 1, we list two possible interloper stars with heliocentric distances shorter than 200 pc. Of them, HD 35926 AB is a binary system separated by 1.3 arcsec (Dommanget & Nys 1994). Additionally, there are other three stars with $d + \delta d < 300$ pc (including errorbars) that we do not classify as possible contaminants. If we fully trust Hipparcos, HD 36429 would be a B5V star at only $d = 200 \pm 30$ pc. The presence of a close companion might have affected its parallax measurement (see, however, Sect. 4.4.4)[4]. Although Briceño et al. (2007) carried out a challenging spectroscopic study of members in Escorial 3 (25 Ori), further analyses in the agglomerate are desirable to disentangle the young star population from the fore-/background and from Ori OB1a and Ori OB1b.

3.2.3 Escorial 4 (η Orionis)

The nine stars in the Escorial 4 agglomerate are located in the southern part of the Ori OB1a subgroup, to the southwest of the Orion Belt. All of them except HD 35957, with a parallactic distance of $d = 190 \pm 40$ pc, seem to be members of the Ori OB1a subgroup based on early spectral types, parallaxes, low proper motions and positions in the V_{T} vs. $B_{\mathrm{T}} - V_{\mathrm{T}}$ colour-magnitude diagram (see also Sharpless (1952) and Warren & Hesser (1978)). To our knowledge, none of the stars have been previously reported to belong to any sub-structure within Ori OB1a. Since the brightest star in the agglomerate is η Ori AB (28 Ori), we propose the name "η Orionis" for the overdensity. Approximate central coordinates and diameter of the overdensity, whose hypothetical cluster nature must be confirmed, are 05 26 30 –01 55 00 (J2000) and 1.2 deg, respectively. From the comparison of cluster photometric sequences, the age of the stars in the η Orionis overdensity must not differ very much from those of the 25 Ori agglomerate and the Orion Belt (e.g. 5–10 Ma).

Briceño et al. (2005) derived the basic properties (T_{eff}, L, M) of the seven single stars in the agglomerate, including HD 35957. Their masses ranged in the interval 2.8–9.4 $M_\odot$. The remaining two stars are in close binary systems, and so it is difficult to derive basic properties from photometry and low-resolution spectroscopy (η Ori AB, $\rho = 1.695$ arcsec; HD 35456 AB, $\rho = 0.810$ arcsec).

See Sect. 4.1.1 for a discussion on the possible cluster nature of the η Orionis overdensity.

3.2.4 Escorial 5 (Orion Sword)

The region of the Orion Sword, including the Trapezium and the Orion Nebula Cluster, is one of the most investigated and scrutinized areas in the sky, and almost does not

---

[3] When available, we follow the Bayer (1603) nomenclature instead of the Flamsteed (1712) one. However, in this case there can be a misunderstanding between 25 Ori (ψ^{01} Ori) and the β Cep-variable star ψ Ori (30 Ori, ψ^{02} Ori).

[4] HD 36429 has a previously unreported companion ($\rho \sim 9.7$ arcsec, $\theta \sim 163$ deg, $\Delta K_{\mathrm{s}} = 3.42 \pm 0.05$ mag), apart from a known visual companion HD 287931 ($\rho \sim 1.1$ arcmin, $\theta \sim 350$ deg, $\Delta K_{\mathrm{s}} = 0.09 \pm 0.03$ mag).

require any introduction (Kwan 1977; Prosser et al. 1994; Hillenbrand 1997; Lada et al. 2000; Feigelson et al. 2002). It is usually presented as "the closest region of massive star formation to the Sun" (although some authors give this honour to the Scorpius-Centaurus association). The four stars that constitute the Trapezium, the asterism that illuminates the Orion Nebula (M 42), are the brightest stars of the Orion Nebula Cluster. This cluster displays the largest stellar density in Orion (together with σ Orionis; see below), and is considered as a distinct subgroup, Ori OB1d. Also in the Orion Sword, and running from north to south, there are other subgroups of extremely young stars that have been classified as members of the Ori OB1c1–4 sub-subgroups (Warren & Hesser 1977). They are differentiated overdensities in the Ori OB1c subgroup. The Orion Nebula Cluster is sandwiched between Ori OB1c3 and Ori OB1c4 sub-subgroups.

Practically all the 23 stars in the Escorial 5 agglomerate have been classified in the literature as members of the Ori OB1c[1–4] or Ori OB1d subgroups (e.g. Parenago 1954; Warren & Hesser 1978). Although it is obvious that the Orion Nebula Cluster has very particular properties (e.g. very high extinction and highly concentrated radial distribution of stars), we have not been able to disentangle it from the remaining stellar population in the Orion Sword (i.e. the Ori OB1c[1–4] sub-subgroups). Indeed, θ^{01} Ori and the Trapezium stars (Hipparcos only identifies three components of θ^{02} Ori) have Tycho-1 $B_T - V_T$ colours redder than –0.05 mag and were not, therefore, in the input catalogue for our DBSCAN algorithm[5]. The brightest and bluest stars in the Escorial 5 agglomerate are ι Ori AC (O9III+, 3 mag-V star in the southern border of M 42), c Ori AB (B1V+, in the centre NGC 1977 nebula, to the north of M 42), HD 36960 (B0.5V, close to ι Ori AC), and υ Ori (B0V, at half a degree to the south of the Trapezium).

3.2.5 Escorial 6 (Orion Belt)

Although the three bright O-type supergiants in the Orion Belt (Alnitak, Alnilam and Mintaka) constitute a prominent asterism in the most obvious constellation in the sky, it was not until late 1920s when Pannekoek (1929) noticed a "clustering of early-type stars elongated roughly parallel to the galactic plane". The three supergiants and dozens young stars in the Orion Belt, *including σ* Orionis, have been considered since Blaauw (1964)'s work to belong to the Ori OB1b subgroup. A complete review of the (sub)stellar populations around the three supergiants is provided in Caballero & Solano (2008). The latter authors describe the Orion Belt as the combination of: (i) a highly extinguished star-forming region surrounding Alnitak (ζ Ori), (ii) a wide, populated, low-density cluster with no clear central overdensity surrounding Alnilam (ϵ Ori), that is spatially coincident with the cluster Collinder 70 (Collinder

1931), and (iii) a recently-discovered cluster candidate surrounding Mintaka (δ Ori).

The 23 stars in the Escorial 6 agglomerate have been previously considered members of the Ori OB1b subgroup (see, again, Warren & Hesser 1978). Our list (Table A1) contains the three supergiants and other well known early-type stars and multiple systems, like the eclipsing spectroscopic binary VV Ori AB, the likely Lindroos system[6] HD 36779 AC–B, or the helium strong, chemically peculiar, variable star V901 Ori. No possible contaminants have been identified. The blue Hipparcos stars in the vicinity of the Horsehead Nebula and the σ Orionis cluster are *not* contained in the Escorial 6 agglomerate (see below).

3.2.6 Escorial 7 (Horsehead)

The Escorial 7 agglomerate contains seven stars, four of which were listed by Caballero (2007) among the brightest stars of the σ Orionis cluster. Both σ Ori AF–B and D (together with the other components of the multiple Trapezium-like system, not catalogued by Hipparcos; Caballero 2008b) are in the centre of the eponym cluster. HD 37525 AB, at 5 arcmin to the southeast of the centre, is still in the "core" of the cluster ($r \leq 20$ arcmin; Caballero 2008a). The last bright cluster member, HD 37699, lies on the "halo" of the cluster, where the contamination by (overlapping) neighbouring young star populations may be large (e.g. Jeffries et al. 2006b). The B1.5V variable star HD 37744, at a bit more than 30 arcmin from the cluster centre, has occasionally been considered as a σ Orionis member (Sherry, Walter & Wolk 2004), but it has not been listed in the recent Mayrit catalogue of stars and brown dwarfs in the cluster (Caballero 2008c). The other (chemically peculiar) two stars, V1148 Ori and HD 37807, are much farther away to the south. The three latter stars (HD 37744, V1148 Ori, and HD 37807) are, besides, spatially coincident with the north-to-south arrangement of the IC 434/NGC 2023 complex, whose more patent structure is the Horsehead Nebula. Because of this coincidence, and of σ Ori illuminating the mane of the Horsehead, we call the Escorial 7 agglomerate "the Horsehead region". Increasing from $R_\epsilon = 0.8$ to 1.0 in our DBSCAN analysis would lead the Escorial 6 (Orion Belt) and 7 (Horsehead) agglomerates to fuse into one subgroup, as commonly considered. In any case, "the Horsehead region" seems to be the juxtaposition of a highly concentrated cluster (σ Orionis), to the northwest, and a younger population of stars associated to the Horsehead Nebula, to the east and southeast.

3.3 The CMa-Pup super-agglomerate

The CMa-Pup super-agglomerate is located to the north of the Canis Majoris-Puppis-Vela region. For an easier description, we have splitted the agglomerates in CMa-Pup

---

[5] The Tycho-2 $B_T - V_T$ colour of the hierarchical triple θ^{01} Ori is, however, bluer than –0.05 mag.

[6] A Lindroos system is a binary with a main sequence, early-type primary and a post-T Tau secondary.
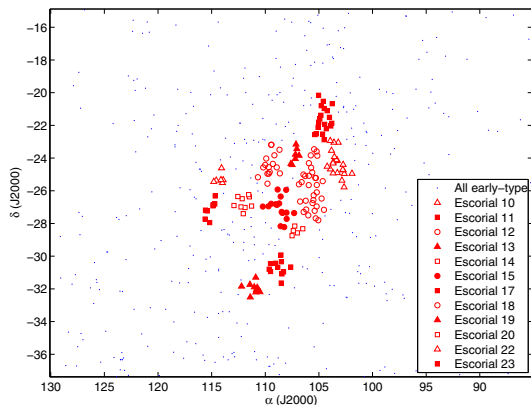
Fig. 7 (online colour at: www.an-journal.org) Same as Fig. 5, but for the agglomerates Escorial 10–15, 17–20, 22, and 23 in the Canis Majoris-Puppis super-agglomerate. The two southern agglomerates (Escorial 17 and 19), at $\delta \leq -30$ deg, belong to the Lower CMa-Pup grouping. The remaining agglomerates belong to the Upper CMa-Pup grouping (the Collinder 121 association).

into two differentiated groupings: "Upper CMa-Pup" (to the north) and "Lower CMa-Pup" (to the south; Fig. 7).

3.3.1 Upper CMa-Pup (Collinder 121)

The Upper CMa-Pup grouping is formed by the agglomerates Escorial 10–15, 18, 20, 22, and 23. Most of the stars in the agglomerates in Upper CMa-Pup except the easternmost Escorial 23 one have been classified as members of the Collinder 121 cluster/association (de Zeeuw et al. 1999; Robichon et al. 1999). According to Kaltcheva & Makarov (2007), Collinder 121 would be the superposition of the genuine compact group discovered by Collinder (1931), which would be at an heliocentric distance of ∼1 kpc, and an extended, loose OB association with a large depth probably extending from ∼0.5 to beyond 1 kpc. Escorial 10, the westernmost agglomerate in the grouping, would be the genuine Collinder 121 cluster (Feinstein 1967).

In total, ten agglomerates are associated to Collinder 121. Given its proximity to the remaining agglomerates, there is no reason to exclude the stars in Escorial 23 from the grouping. This is the first time in the literature to propose such a drastical division of Collinder 121. The extension of the region, of up to 12 deg in both vertical and horizontal directions, would lead to maximum physical separations between stellar components of 100–200 pc. This size is not far larger than that estimated for the Orion complex (Sect. 3.2), which we have splitted into 5+1 agglomerates. Upper CMa-Pup/Collinder 121 might be an analog to the Orion complex, but at a triple heliocentric distance and splitted into ten agglomerates. The grouping contains the most populated agglomerate, Escorial 12 ($N_\star$ = 32, roughly centred on the blue supergiant 24 CMa)[7]. There

[7] Star 24 CMa is o^{02} CMa; do not mistake with 16 CMa (o^{01} CMa, K2.5Iab:).

are also some Upper CMa-Pup stars in known open clusters that could be associated to Collinder 121, or be in the background (e.g. NGC 2362 surrounding τ CMa AB in Escorial 18 – age = 5^{+1}_{-2} Ma, d = 1480 pc; Moitinho et al. 2001). Some stars are associated to reflection nebulae (e.g. HD 61071 in Escorial 22; van den Bergh 1966).

In Table A1, we list four possible contaminants in the foreground of Upper CMa-Pup/Collinder 121. All of them have parallaxes and/or proper motions inconsistent with membership in the association (the Hipparcos measurements of m Pup AB could be affected by close binarity – actually, it could be a hierarchical triple system, since the primary is thought to be a eclipsing binary; Stift 1979). It is interesting to notice the very early spectral types of some of these interlopers, like the well-known, emission-line, variable star ω CMa (B2IV/Ve – Baade 1982; Sletteback 1982; Štefl et al. 2003), which is located at only d = 279±13 pc according to van Leeuwen (2007a).

3.3.2 Lower CMa-Pup: Escorial 17 (Collinder 132) and 19 (Collinder 140)

There remain two agglomerates in the CMa-Pup super-agglomerate: Escorial 17 and 19. They are associated to Collinder 132 and 140, respectively, and form the Lower CMa-Pup grouping. Each of the agglomerates has only one possible foreground contaminant (Table A1).

There has been only one dedicated work in Collinder 132, carried out by Clariá (1977), and there still remain caveats on the actual nature and structure of the cluster. First, Clariá (1977) interpreted that there are two separate physical groups, called "Cr 132a" and "Cr 132b", located at 560 and 330 pc from the Sun, and with nuclear ages of 60 and 160 Ma, respectively. Eggen (1982) and Baumgardt (1998) supported the double cluster hypothesis, but with nuance. Baumgardt (1998) stated that "Collinder 132 is found to be mainly composed out of members of an OB association, but there may be a star cluster present in this area too". He also proposed that there may be a connection between Collinder 132 and Upper CMa-Pup/Collinder 121. However, Robichon et al. (1999) derived a unique parallactic distance of d = 650±140 pc, much further away than the 270 pc tabulated by Wielen (1971), who took the value, in its turn, from Collinder (1931). Other authors have catalogued closer distances ($d \approx 400$ pc) and younger ages (∼25 Ma; e.g. Battinelli, Brandimarti & Capuzzo-Dolcetta 1994).

Our Escorial 17 agglomerate possesses 11 stars. The Collinder 132 cluster centre has been considered to fall close to the brightest star in our agglomerate, HD 56342 (B3V). Indeed, this star was classified as the brightest cluster member by Clariá (1977). HD 56342 has, however, parallax and proper motion measurements clearly different from the rest of the stars of the agglomerate. This difference led us to classify it as a young contaminant star in the foreground. Obviously, an isolated bright B3V dwarf at

only $d = 193\pm8$ pc is very uncommon; it will be discussed in Sect. 4.4.4. From our data, we identify only one structure with heliocentric distance and age consistent with those provided by Robichon et al. (1999) ($d = 650\pm140$ pc) and Battinelli et al. (1994) (age ~ 25 Ma). There might be a cluster of *faint* stars in the foreground, associated to HD 56342, but we fail to identify it.

Collinder 140, although discovered by Collinder (1931), could have been previously identified by de Lacaille (1755), who gave it the name "Nebulous Star Cluster No. II.2" (*aka* Lacaille II.2). Since Collinder 140 contains at least five stars brighter than $V = 7$ mag in a concentrated arrangement, the cluster has received a larger attention than Collinder 131. Williams (1967a, 1978), Fitzgerald, Harris & Miller (1980), Lyngå & Wramdemark (1984), and other authors have investigated Collinder 140 in detail. Williams (1967b) suggested that Collinder 140 and NGC 2451 (Sect. 3.4.3), together with other two open clusters, are "the remaining nuclei of an OB association" that broke up. Clariá & Rosenzweig (1978) carried out the most complete investigation in Collinder 140. They derived its heliocentric distance ($d = 365\pm29$ pc), nuclear and contraction ages (at about 20–25 Ma), physical size (~ 10 pc), total mass ($\geq 100 \, M_\odot$), number of evolved members (≥ 3), metallicity ([Fe/H] $= -0.1$), and other parameters, like the cluster radial velocity or the Galactic space motion. Different heliocentric distances and ages have been provided afterwards (Williams 1978: $d = 420\pm20$ pc, age ~ 40 Ma; Fitzgerald et al. 1980: $d = 410\pm30$ pc, age $= 20\pm6$ Ma – they pointed out a significant concentration of yellow giants; Robichon et al. 1999: $d = 410^{+60}_{-40}$ pc).

One of the brightest stars in Collinder 140 is the variable supergiant HD 58535 (G8II, $V = 5.35$ mag – Harris 1976; Clariá 1976). It has a very red $B_T - V_T$ colour and was not in the input catalogue of our DBSCAN algorithm. The rest of the Hipparcos stars in Escorial 19 have also been classified as members of Collinder 140, except for the binary HD 59499+HD 59500 (B3V+B4V), that lies at about 1 deg to the east of the cluster centre. We classify the binary as a Collinder 140 candidate member for the first time. Robichon et al. (1999) listed other three Hipparcos stars with $B_T - V_T > -0.05$ mag that are not, therefore, in our compilation. Besides, we have classified the EA-type eclipsing binary HD 58285 (B9III, $P = 2.198515$ d, in eccentric system – Houk 1982; Otero & Dubovsky 2004) as a possible contaminant in the outer part of Collinder 140, because of its distinguishable proper motion. The weighted mean heliocentric distance to Collinder 140, from our Hipparcos data, is $\overline{d} = 370\pm50$ pc. It is similar to the distance measured by Clariá & Rosenzweig (1978), and consistent within errorbars with other recent determinations.

3.4 The Pup-Vel super-agglomerate

The Pup-Vel super-agglomerate is, as well as CMa-Pup, in the Canis Majoris-Puppis-Vela region. However, although
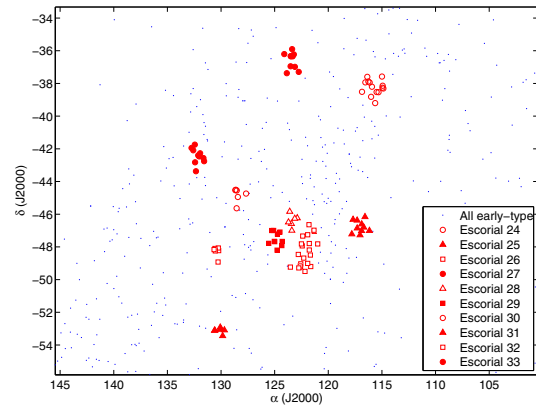
Fig. 8 (online colour at: www.an-journal.org) Same as Fig. 5, but for the agglomerates Escorial 24–33 in the Puppis-Vela super-agglomerate. The trio Escorial 26–28 is in the centre; Escorial 30, IC 2391 (Escorial 31), IC 2395 (Escorial 32), and Trumpler 10 (Escorial 33) are to the east; NGC 2451 AB (Escorial 24) and vdBH 23 (Escorial 27) are to the north; and Escorial 25 is to the west.

our DBSCAN algorithm has also splitted it into ten agglomerates, the Pup-Vel super-agglomerate is not as compact as the CMa-Pup one. The ten agglomerates in Pup-Vel are distributed in a hierarchical spatial distribution. The largest spatial density coincides with a dense part of the Vel OB2 association (Sect. 3.4.1). Surrounding this "core", there are other seven well-defined clusters, some of which have been repeatedly investigated in the literature (IC 2391, Trumpler 10, and NGC 2451 AB).

3.4.1 Escorial 26, 28, and 29

Escorial 26, 28, and 29 form a dense trio of agglomerates, usually ascribed to the Vel OB2 association. The largest and most populated agglomerate is Escorial 26, that has an elongated shape in the north-south direction. Although our DBSCAN algorithm has not been able to disentangle both populations, the Escorial 26 agglomerate is actually the juxtaposition of the γ Velorum star-forming region, to the north, and the NGC 2547 cluster, to the south. The open cluster Collinder 173 is at the northern borderline of the agglomerate.

On the one hand, the γ Velorum region practically coincides with the densest part of the Vel OB2 association, that was identified by Kapteyn (1914) and described in detail by de Zeeuw et al. (1999)[8]. The (at least) sextuple γ Vel star (γ^{02} Vel) is in the centre of the association, and is one of the brightest stars in the nighttime sky ($V \approx 1.8$ mag). The brightest component of γ Vel is actually a spectroscopic binary composed of WR 11 (WC8), the nearest known Wolf-Rayet star, and a massive O9I supergiant with a 78.5-day orbital period. An heliocentric distance of 411 ± 12 pc was

---

[8] Do not mistake with Eggen (1982)'s Vel OB2, that corresponds to another group of stars.

derived by de Zeeuw et al. (1999). They also listed literature ages in the interval 6–20 Ma. Interestingly, the Vela Pulsar was born in Vel OB2 about 10^4 a ago (Hoogerwerf, de Bruijne & de Zeeuw 2001). On the other hand, NGC 2547 has been very well investigated. The cluster is very important for studying X-ray emission (Jeffries & Tolley 1998; Jeffries et al. 2006a), the Wielen dip[9] (Naylor et al. 2002), the lithium depletion boundary (Jeffries & Oliveira 2005), the disc frequency (Young et al. 2004; Gorlova et al. 2007), low-mass stars and brown dwarfs (Jeffries et al. 2004), mass segregation (Littlefair et al. 2003), and rotation and activity (Jeffries, Totten & James 2000; Irwin et al. 2008). It is 30±10 Ma old (see Oliveira et al. (2003) for a discussion on the discrepancy between ages from isochrone fitting and from the lithium depletion boundary) and at 400–450 pc, and has a low reddening (Fernie 1959, 1960; Clariá 1982 and references above). In Table 1, we list three possible contaminants in the Escorial 26 agglomerate (HD 68657, at $d = 259\pm18$ pc and with a distinct proper motion, has an early spectral type B3V, according to Hiltner, Garrison & Schild 1969. It might be a B-type subdwarf in the foreground).

The other 16 stars in the trio are located to the east and northeast of Escorial 26, overlapping with the Vela supernova remnant. They are distributed among two agglomerates: Escorial 28 (northeast, $N_\star = 6$) and Escorial 29 (east, $N_\star = 10$). HD 70251 could be a foreground interloper in the latter agglomerate (it is a B8V stars at $d = 290\pm30$ pc and discordant proper motion). Most of the remaining stars have been classified as members of the Vel OB2 association. Remarkably, HD 70309 A (B3III) is the primary of a Lindroos system (the secondary, HD 70309 B, is a K2IV star – Lindroos 1985; Pallavicini, Pasquini & Randich 1992).

To sum up, we find evidence of subclustering in Vel OB2. Besides, the similarity in heliocentric distance and age between Vel OB2, γ Velorum, and NGC 2547 may suggest that they actually belong to the same complex, but NGC 2547 having a much larger spatial density of members.

3.4.2 Escorial 30, 31 (IC 2391), 32 (IC 2395), and 33 (Trumpler 10)

The four agglomerates Escorial 30–33 are located to the east of the Pup-Vel super-agglomerate, rather separated between them and from the core of the Vel OB2 association formed by the trio of agglomerates described in Sect. 3.4.1.

Escorial 30 might be a spurious agglomeration: three of the six stars in the agglomerate have been classified as members of the concentrated, elongated Pismis 4 cluster (Moffat & Vogt 1975; Baumgardt et al. 2000), while the other three neighbouring early-type stars seem to populate the outskirt of Pismis 4 and belong to the Vel OB2 association, or even to other open clusters in the surrounding area (e.g. HD 72350 AB in the van den Bergh-Hagen 34 [vdBH 34]

cluster; Dias et al. 2001). From our data and from Moffat & Vogt (1975)'s, the Pismis 4 cluster is located at 500–600 pc to the Sun, in the background of the Vel OB2 association.

IC 2391 is, as well as the Pleiades, the Orion Nebula Cluster, σ Orionis, or NGC 2547, a cornerstone for the study of the formation and evolution of stars and substellar objects at all mass domains (Hogg 1960; Perry & Hill 1969; Stauffer et al. 1989, 1997; Patten & Simon 1996; Barrado y Navascués, Stauffer & Jayawardhana 2004; Boudrealt & Bailer-Jones 2007; Siegler et al. 2007). Besides, Koester & Reimers (1985) found a white dwarf in the cluster (IC 2391 KR 1 [WD 0839–528]), that could be the youngest one yet found, together with other white dwarfs identified towards NGC 2451 (that is described in Sect. 3.4.3). See also Platais et al. (2007) for recent improvements of the basic parameters of IC 2391 ($d = 159.2$ pc, age ~ 40 Ma, [Fe/H] = +0.06). The seven stars in the Escorial 31 agglomerate are bright, classical members in the cluster. The brightest stars in IC 2391 are o Vel (B3IV, $V = 3.60$ mag) and HY Vel (B3IV, $V = 4.83$ mag). In Sect. 4.4.3 we derive a new heliocentric distance to the cluster.

Four of the six stars in the Escorial 32 agglomerate were classified as members of the IC 2395 (vdBH 47, Collinder 192) cluster. Of the remaining two stars in agglomerate, one (HD 74273) is well separated (by almost 1 deg) from the relatively concentrated cluster and may belong to a different young population in the area, while the other one (HD 74531 A) has magnitudes, colours, and spectral type (B2V:) that match the IC 2395 spectro-photometric sequence. The cluster had been poorly investigated (Lyngå 1960, 1962; Ruprecht 1966; van der Bergh & Hagen 1975; Jørgensen & Westerlund 1988) until the clarifying work by Clariá et al. (2003). They derived the angular size ($\sim$19 arcmin), heliocentric distance ($d = 800\pm40$ pc), and age (6 ± 2 Ma) of IC 2395, and suggested a physical connection to the Vel OB1c association (Mel'nik & Efremov 1995). We can not provide additional information or improvement from our data. The brightest star in IC 2395, that may define the cluster centre, is the binary ($\rho \approx 0.3$ arcsec), variable, early-type (B1.5V + mid-B) star HX Vel.

Six of the 10 stars in the Escorial 33 agglomerate were listed as genuine Trumpler 10 *cluster* members by Lyngå (1960, 1962), while one of the four remaining stars was also listed as a Trumpler 10 *association* member by de Zeeuw et al. (1999). According to the latter authors, Trumpler 10 (vbBH 53) is not "a tight open cluster, but instead an intermediate age OB association". However, the association/cluster nature of Trumpler 10 is not well understood yet. On the one hand, Lyngå tabulated a diameter of only 14 arcmin for the cluster; this value contrasts with the $\sim$8 deg estimated by de Zeeuw et al. (1999) for the association. The doubt of the "entity" being a single cluster had been firstly proposed by Stock (1984)[10]. Although

---

[9] The Wielen dip is a feature in the luminosity function at $M_V \approx 7$–8 mag. NGC 2547 is the youngest open cluster to display it.

[10] There are additional foreground open clusters at less than 1 deg to the highest star concentration of Trumpler 10. NGC 2671 is an $\sim$80 Ma-old cluster at $d \sim 1700$ pc (Pedreros 2000). ESO 260–8 is an ultracompact

the original Lyngå's clustering of bright stars is evident in digitized plates (see Fig A11), the mean heliocentric distance to the sparse association computed by de Zeeuw et al. (1999; $d = 366\pm23$) is consistent with previous determinations of distance to the cluster (Levato & Malaroda 1975a; Eggen 1980; Lyngå & Wramdemark 1984). The identification of the Escorial 33 agglomerate also supports the existence of an OB association of age ~15 Ma in the area, whose densest part would be the original Lyngå's cluster. Finally, Kaplan, van Kerkwijk & Anderson (2007) measured the parallactic distance to the isolated neutron star RX J0720.4–3125 ($d = 360^{+170}_{-90}$ pc), and suggested an origin for it in the Trumpler 10 association $0.7^{+0.2}_{-0.2}$ Ma ago. Escorial 33/Trumpler 10 deserves further analyses on its stellar content and basic properties (age, distance, spatial distribution, mass function).

3.4.3 Escorial 24 (NGC 2451 AB) and 27 (vdBH 23)

The northernmost agglomerates in the Pup-Vel super-agglomerate, roughly equidistant from the maximum star densities of CMa-Pup and Pup-Vel, are Escorial 24 and 25.

Escorial 24 is associated to NGC 2451 AB, which is actually the superposition of two clusters at different heliocentric distances. First catalogued by Dreyer (1888), NGC 2451 is one of the ten closest open clusters to the Sun (see Hünsch, Weidner & Schmitt 2003 for a historical review). It was firstly studied in detail (as a single cluster) by Feinstein (1966) and in a series of papers by Williams (1966, 1967b). Prior to 1990, it was revisited by Levato & Malaroda (1975b) and other authors (Andersen & Reiz 1983; Eggen 1983; Pastoriza & Ropke 1983; Maitzen & Catalano 1986; Gilroy 1989). There have been later studies in NGC 2451 on close resolved photometry (Platais et al. 2001), photometry and membership (Carrier, Burki & Richard 1999), X-ray emission (Hünsch et al. 2003), and rotation and lithium abundance (Hünsch et al. 2004). The "binary" status of NGC 2451 A and B has also been confirmed by many authors (Baumgardt 1998; Röser & Bastian 1994, and references above). Robichon et al. (1999) derived $d = 188.7^{+7.0}_{-6.5}$ pc for NGC 2451 A, and determined an age of 35–55 Ma, consistent within error bars with the more recent determination by Platais et al. (2001; 60 ± 20 Ma) and Hünsch et al. (2003; 56–80 Ma). NGC 2451 A could be the core of a moving group (the Puppis Moving Group – Röser & Bastian 1994). NGC 2451 B is of a similar age but, in contrast, located further away. Carrier et al. (1999) derived $d = 358\pm22$ pc for NGC 2451 B. These authors also investigated in detail the exceptional emission-line star V468 Pup (B6IVe).

Our list of 14 stars in Escorial 24 approximately match other lists of bright blue stars in NGC 2451 (both A and

B). However, we classify the stars in Escorial 24 in three groups:

- 10 star members in NGC 2451 A, with mean proper motion $(\overline{\mu_\alpha\cos\delta}, \overline{\mu_\delta}) = (-21.3\pm1.7, +15.4\pm1.0)$ mas a^{-1} and heliocentric distance $\overline{d} \leq 200$ pc (see Sect. 4.4.2);
- three star members in NGC 2451 B (HD 61899[11], HD 62991, and HD 63465), with mean proper motion $(\overline{\mu_\alpha\cos\delta}, \overline{\mu_\delta}) = (-10.2\pm0.4, +7\pm3)$ mas a^{-1} and heliocentric distance $\overline{d}$ 340$\pm$30 pc; and
- star V468 Pup, with $d = 430\pm40$ and $(\mu_\alpha\cos\delta, \mu_\delta) = (-0.84\pm0.18, -4.4\pm0.2)$ mas a^{-1}. This star, although it was considered as a NGC 2451 B member by Carrier et al. (1999), has discordant proper motion and heliocentric distance, and belongs to a *third* background stellar population.

To sum up, the Escorial 24 agglomeration is the superposition of at least two young open clusters. The brightest star in the area, c Pup AB (a K2.5Ib-II star in NGC 2451 B), has a colour $B_T - V_T = 2.038\pm0.017$ mag and was not, therefore, in the input catalogue of our DBSCAN algorithm. Based on proper motion and parallax analysis, we confirm non-membership in NGC 2451 A or B of the bright ($V = 6$–8 mag) stars HD 62559 (F2IV), HD 63738 (F7V), and HD 63291 (K3II–III). Besides, HD 62595 is a G7III star that probably belong to NGC 2451 B. The four Hipparcos stars also have colours $B_T - V_T > -0.05$ mag.

Likewise, the Escorial 27 agglomerate contains 11 stars. The two brightest ones are the B1.5-type giant MX Pup[12] and the dwarf OS Pup. The agglomerate is to the north of the NGC 2546 cluster and in southeastern vicinity of the H II region Gum 10 (Gum 1955; Rodgers, Campbell & Whiteoak 1960). It was Westerlund (1963) who firstly indicated the existence of an OB association in the region of the long-period cepheid RS Pup (F8Ia), that is relatively close to Escorial 27. This association, now called Pup OB3, is very wide and contains most of the stars in our agglomerate. He estimated an age of only 4 Ma, consistent with the observed spectral types and apparent magnitudes. Later, van den Bergh & Hagen (1975) reported a not previously catalogued cluster roughly centred on OS Pup. This cluster, van den Bergh-Hagen 23 (vdBH 23), had quite uncertain parameters until was rediscovered in more recent works (Platais et al. 1998; Kharchenko et al. 2005). An heliocentric distance of $d \sim 384$ pc was estimated by Dias et al. (2001). Although not all the stars in the Escorial 27 agglomerate have been catalogued as members of vdBH 23, they probably represent the same entity. The O9.5II supergiant HD 68450 is probably a star in the background and does not belong to Escorial 27/vdBH 23. From the weighted mean of the parallaxes of the remaining ten stars, we derive an heliocentric distance of $\overline{d} = 320\pm30$ pc, slightly lower than

---

H II region, apart from a radio (methanol maser) and IRAS source, at $d \sim$ 1.3 kpc (Griffith & Wright 1993; Walsh et al. 1997; Dutra et al. 2003).

[11] We use the Henry Draper nomenclature instead of d^{03} Pup, since it is easy to misunderstand with d^{02} Pup (HD 61878 AB), that belongs to NGC 2451 A.

[12] We use the variable star name MX Pup instead of r Pup, since it is easy to misunderstand with R Pup (an F9Ia supergiant in NGC 2439).

Dias et al. (2001)'s estimation. A dedicated study of Escorial 27/vdBH 23 is still to be carried out.

3.4.4 Escorial 25 (P Puppis)

Most of the ten stars in the Escorial 25 agglomerate are poorly known. Three of them are the β Cep variable QS Pup and the very bright giants P Pup AC and HD 63578 (V = 4.10 and 5.22 mag, respectively). The latter star and other two ones in the agglomerate (HD 63343 and HD 63449 AB, a close double with ρ = 0.496 arcsec) were classified as members of the Vel OB2 association by de Zeeuw et al. (1999). Apart from photometry and astrometry, there is no additional information for the remaining stars.

The region displays an evident larger surface density of early-type stars than in its surroundings, and it is located at a considerable angular separation from the Vel OB2 trio of agglomerates (Sect. 3.4.1). Escorial 25 probably belongs to the Pup-Vel super-agglomerate, but not to the "core" of Vel OB2. We propose for the first time the existence of an open cluster coinciding with Escorial 25, approximately centred on P Pup AC, the brightest star in the agglomerate. Therefore, we call it the "P Puppis cluster". The ten Hipparcos stars in Escorial 25/P Puppis delineate a sharp cluster sequence in the B_T vs. $B_T - V_T$ colour-magnitude diagram. HD 63007 (B5V) has, however, proper motion and heliocentric distance slightly different from the remaining cluster member candidates; HD 63007 might be, therefore, a foreground contaminant. Accounting for the remaining nine Hipparcos stars in the cluster, if confirmed, it would be located at an heliocentric distance of $\overline{d}$ = 470±70 pc.

The only very bright, red star in the area is the evolved giant Q Pup (K0III), with heliocentric distance and proper motion inconsistent with membership in Escorial 25/P Puppis (d = 70±2 pc, μ > 100 mas a^{-1}). As a result, there is no evidence of cluster stars in the Red and Asymptotic Giant Branches. The brightest star in the cluster is an early-type giant (B0III) that has not moved away from main-sequence. The same can be applied to the subgiants QS Pup and HD 63578 (B1.5IV). The next stars in brightness order are B3–5V dwarfs, that have evolutionary ages of roughly 20 Ma. We will assume a very young age of 10^{+10}_{-5} for the P Puppis cluster.

Further analyses, required to ascertain the nature of Escorial 25/P Puppis, will be presented in Sect. 4.1.2.

4 Discussion

4.1 Two new clusters: η Orionis and P Puppis?

4.1.1 η Orionis

Among the 35 identified agglomerates, two of them have never been proposed to be real clusters (i.e. their stars are gravitationally bound). They are the η Orionis overdensity and the P Puppis cluster candidate.

As already mentioned in Sect. 3.2.3, the centre of the η Orionis overdensity does not coincide with the massive (double) star η Ori AB. In order to avoid the limits of the Hipparcos catalog and our colour selection, we carried out a new Virtual Observatory analysis of the region. In particular, we loaded with Aladin all Tycho-2 stars at less than 2 deg to the central coordinates in Sect. 3.2.3 (N = 734), and selected all of them with colours $B_T - V_T$ < +0.25 mag and magnitudes V_T < 10.50 mag (N = 96). We checked that all the selected stars have very low proper motions ($\mu \leq$ 10 mas a^{-1}) and follow a relatively narrow sequence in the B_T vs. $B_T - V_T$ colour-magnitude diagram, consistent with its membership in Orion, and that redder non-selected stars of similar brightness have colours (and parallaxes) typical of field dwarfs in the foreground.

We counted the number of selected stars in coronae centred on both η Ori AB and the survey area central coordinates, and did not find a clear evidence of a *dense* star agglomeration as has been found in other sites in Ori OB1 (like in the Orion Nebula Cluster and the σ Orionis cluster). Besides, the elongated shape of the overdensity gets more patent with the Tycho-2 data, which contrasts with the symmetrical, radial density gradient found in well-characterized clusters (Cartwright & Whitworth 2004; Caballero 2008a). To sum up, we confirmed that a spread overdensity of bright, early-type stars does exist in the area of η Ori AB in the Ori OB1a association. However, we failed to corroborate the existence of a (gravitationally bound) cluster in that region.

4.1.2 P Puppis

We followed a similar procedure to that of the η Orionis overdensity in the previous section for studying the possible cluster nature of the agglomerate Escorial 25/P Puppis. First, we selected all Tycho-2 stars satisfying the colour and magnitude restrictions listed above. In this case, we only loaded the stars in a 90 arcmin-radius circle centred on P Pup AC. The photometric sequence in the colour-magnitude diagram in top left panel of Fig. 9 is very sharp, as already noticed in Sect. 3.4.4 with the Hipparcos data. Remarkably, the three brightest stars in the agglomerate (i.e. the two resolved components in P Pup AC and the subgiant QS Pup) lie on a circle with a radius of only 45 arcmin, which subtends and area four times smaller than the 90 arcmin-radius circle. Far from expecting four times less blue, bright stars, approximately half of them are within the smaller radius (i.e. there are twice more blue bright stars in the inner circle than expected – the deviation is at the level of five times the square root of the Poissonian variance), suggesting a *dense* star agglomeration.

We probed the very low-mass stellar population (close to the substellar boundary) in the 45 arcmin-radius circle using the Dee Near Infrared Survey of the Southern Sky (DENIS; Epchtein et al. 1997) and the Two-Micron All Sky Survey (2MASS; Skrutskie et al. 2006) and the NextGen98 theoretical isochrones of Baraffe et al. (1998). We proceed
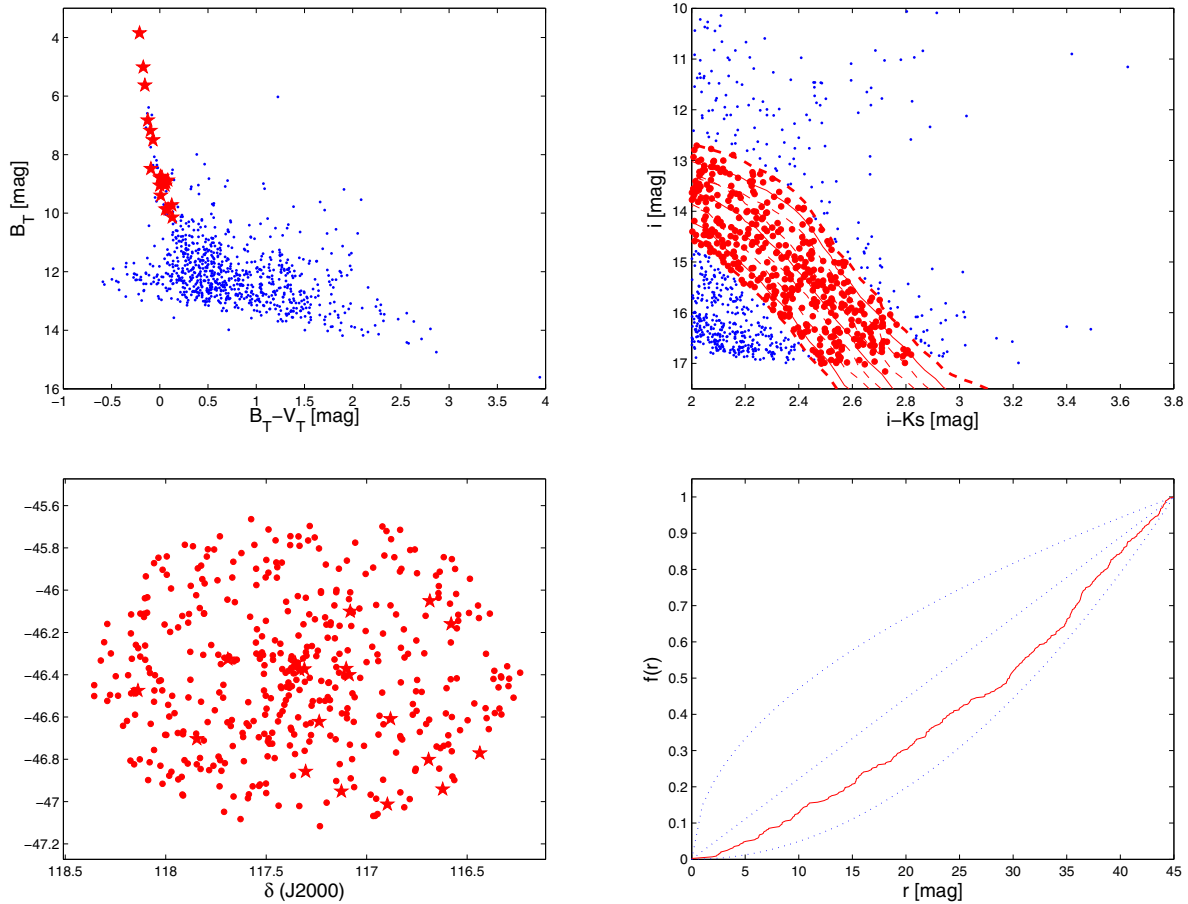
Fig. 9 (online colour at: www.an-journal.org) Some diagrams illustrating the follow-up of the P Puppis cluster. *Top left*: B_T vs. $B_T - V_T$ colour-magnitude diagram showing Tycho-2 cluster member candidates at less than 45 arcmin to P Pup AC (filled red stars) and remaining objects at up to 90 arcmin to the early-type binary (small blue dots). *Top right*: the faintest, reddest portion of the i vs. $i - K_s$ diagram showing DENIS/2MASS cluster member candidates at less than 45 arcmin to P Pup AC (filled red circles) and remaining objects at the same angular separation (small blue dots). Solid (red) lines are for the 5, 10, and 20 Ma-old NextGen98 isochrones (from top to bottom) shifted at $d = 470$ pc, while dashed (red) lines are for the previous isochronesess shifted at $d = 400$ (above) and 570 pc (below). *Bottom left*: spatial distribution of the Tycho-2 (filled stars) and DENIS/2MASS (filled circles) cluster member candidates. *Bottom right*: normalized cumulative number, $f(r)$, of cluster member candidates, in solid (red) line, and theoretical power-law distributions for $f(r) \propto r^{1/2}$, r^1, and r^2 (from top to bottom). Compare with figures in Caballero (2008a).

as in Caballero & Solano (2008), by loading DENIS and 2MASS data and cross-matching the sources. We filtered the faintest ($i > 10$ mag), reddest ($i - K_s$) sources with the highest quality photometry (δi, δJ, δH, $\delta K_s < 0.1$ mag). Since the Virtual Observatory selection of P Puppis cluster member candidates cannot be carried out through the definition of a lower envelope of spectroscopically confirmed young stars (as in the σ Orionis; Caballero 2008c) or of a redder envelope that both maximizes the number of cluster members and minimizes the number of contaminants (as in the Alnilam/Mintaka region; Caballero & Solano 2008), we opted for the classical selection criterion based on theoretical isochrones. As can be seen in the colour-magnitude diagram in top left panel in window Fig. 9, the theoretical P Puppis sequence, considering all possible uncertainties in the cluster heliocentric distance ($d = 470 \pm 70$ pc) and age (10^{+10}_{-5} Ma), is quite broad and overlaps with the location

of a lot of (foreground) field M-type dwarfs. Other colour-magnitude diagrams, performed with the same technique in regions of exactly the same area and galactic latitude, and of approximately the same galactic longitude, are quite similar, which indicates that many of the selected cluster member candidates (between the 5 Ma, 400 pc and the 20 Ma, 540 pc NextGen isochrones) are actually late-type interlopers. Although some elaborated de-contamination technique could be applied (e.g. Caballero, Burgasser & Klement 2008), a central overdensity of selected cluster members is already obvious (see the spatial distribution of selected sources in the bottom left panel in Fig. 9). Since there are 425 DE-NIS/2MASS selected sources in the 45 arcmin-radius circle, one should expect ~100 such objects in the four-times smaller area defined by a 22.5 arcmin-radius circle centred on P Pup AC. In contrast, we found more than 150 of them. In other words, there are at least ~50 (young) low-mass

stars at less than 20–25 arcmin to the B0 giant that probably form part of the P Puppis cluster.

Other way of illustrating the central overdensity of P Puppis is the diagram of the normalized cumulative number of cluster member candidates, $f(r) = N(r)/N(r_{max})$, as a function of angular distance to the the centre, r. A wealth of details on how to compute and interpret it are in Caballero (2008a). In short, a power-law distribution $f(r) \propto r^2$ corresponds to a uniform distribution of objects in the survey area, while $f(r) \propto r^1$ corresponds to a volume density proportional to r^{-2}, which is consistent with the collapse of an isothermal spherical molecular cloud (e.g. Burkert, Bate & Bodenheimer 1997). A distribution with an intermediate index, as that one observed in the Mintaka cluster (Caballero & Solano 2008) and in P Puppis from $r = 0$ to $\sim$25 arcmin (bottom right panel in Fig. 9) corresponds to the superposition of a radially-concentrated cluster with $f(r) \propto r^1$ and a homogeneously-distributed population of (late-type, field dwarf) contaminants.

To sum up, we discover a star cluster surrounding the young, massive P Pup AC giant. However, a dedicated spectroscopic follow-up will be necessary to disentangle between the stellar populations of the cluster and of the field.

4.2 New sites for substellar searches

Some of the agglomerates identified in our work are valuable "hunting grounds" for the search of faint brown dwarfs and planetary-mass objects. In particular, the first brown dwarf, Teide 1, was found in the Pleiades cluster (Rebolo et al. 1995), while the Orion Nebula and the σ Orionis clusters harbour the great majority of the planetary-mass objects with spectroscopy (Lucas & Roche 2000; Zapatero Osorio et al. 2000). Other listed agglomerates that have held substellar searches are the Orion Belt (surrounding Alnilam and Mintaka), NGC 2264, NGC 2547/γ Velorum, and IC 2391. However, there are agglomerates in our list that share properties (youth, closeness, low extinction) that also make them ideal sites for substellar searches.

After discarding the possible spurious agglomerates and the groupings associated to Collinder 121 and Vel OB2, that are too far away and/or too sparse for efficient searches, we retained 14 agglomerates for a follow-up inspection of their parameters. Of them, five seem to be at prohibitive heliocentric distances larger than 650 pc (i.e. NGC 2353, Collinder 132, NGC 2362, Pismis 4, and IC 2395). Besides, M 47, although being located at $d \sim 470$ pc, has a Pleiades-like age and, therefore, their hypothetical brown dwarfs will be about 3 mag fainter.

We maintain eight agglomerates as new sites for substellar searches. Two of them are obvious choices, because they resemble their "elder brothers" (in contraposition to "fraternal twins") in Orion: 25 Orionis and η Orionis. Even in the case that η Orionis is not a real cluster, the large observed stellar surface density will facilitate forthcoming studies

(stellar and substellar objects are expected to have proportional surface densities; Caballero 2008a). NGC 2451 A, with an age of $\sim$45 Ma and a very close heliocentric distance of $d = 180$–200 pc (see Sect. 4.4.3) is other apparent option.

If compiled basic data for vdBH 23 (Escorial 27) and Trumpler 10 (Escorial 33), with distances and ages in the approximate intervals 320–360 pc and 1–4 Ma, are correct, then they might be new cornerstones for the substellar searches in the near future. Finally, there remain in order of interest, NGC 2232 (Escorial 8; $d \sim 320$ pc, age ~ 30 Ma), Collinder 140 (Escorial 19; $d \sim 370$ pc, age ~ 20 Ma), and our new cluster P Puppis (Escorial 25; $d \sim 470$ pc, age ~ 10 Ma). The first two clusters in the trio seem to be IC 2391 twins at larger distances, while P Puppis resembles the stellar groupings in the Orion Belt.

4.3 Sub-structure of super-agglomerates

We find evidence of spatial sub-structure within classical OB associations. First, the "isolated cluster" Escorial 35 could be a physical grouping within Lac OB1 (Sect. 3.1.6). Secondly, our three super-agglomerates (Orion, CMa-Pup, and Pup-Vela) are, by definition, the combination of a number of individual agglomerates. There can be sub-sub-structure (i.e. sub-structure within the agglomerates), as described in, for example, Sects. 3.1.3 (NGC 2264), 3.2.5 (Orion Belt), and 3.4.3 (NGC 2451 AB), but it was not our aim to detect it.

The Orion super-agglomerate is composed of five agglomerates, whose boundaries do *not* coincide with classical divisions within the Ori OB1 complex. The Orion Sword (Escorial 5) is the superposition of 23 stars previously ascribed to the sub-associations Ori OB1c[1–4] and Ori OB1d, and includes the brightest stars of, e.g., the Orion Nebula Cluster. The Orion Belt (Escorial 6) coincides with Ori OB1b, except for the fact that it does not contain the stars in the nearby σ Orionis cluster, that form the largest spatial overdensity in a new agglomerate of early-type stars close to the Horsehead Nebula (Escorial 7). Finally, we identify two agglomerates surrounding the very bright stars 25 Ori (Escorial 3) and η Ori (Escorial 4) in the Ori OB1a sub-association. While the 25 Ori agglomerate was identified very recently, we report here for the first time the existence of a possible open cluster surrounding η Ori.

The classical view of sequential formation of subgroups in OB associations by Elmegreen & Lada (1977) is reinforced by our results. As shown in Fig. 6, the stars in the Orion super-agglomerate are aligned in the north-south direction. Noticeably, the oldest (or less young) agglomerate is located northward (25 Ori; $\sim$10 Ma), the youngest one southward (Orion Sword; $\sim$1 Ma), and those ones with intermediate ages (Orion Belt, Horsehead, and, possibly, η Ori) in the middle. Extrapolating backward, it might happen that the λ Orionis cluster (to the north of the Orion super-agglomerate) is older than 25 Ori. On the other hand,

the ionization and front shocks produced in the Orion Sword might also initiate in the near future another cycle of OB star formation to the south of Orion, where large concentrations of molecular gas have been detected by the IRAS satellite.

We have broken up the CMa-Pup super-agglomerate into Collinder 132 (Escorial 17) and Collinder 140 (Escorial 19) to the south and Collinder 121 to the north. Collinder 121 has been splitted, in its turn, into ten agglomerates. One of them, Escorial 10, would be the original Collinder 121 compact group that gives the name to the extended, loose OB association. The few dedicated spectro-photometric analyses in the region do not allow to conclude if there are younger and older regions within the super-agglomerate. The spatial sub-structure suggests, however, that Collinder 121 is an analog to the Ori OB1 association at about 1 kpc to the Sun.

The Pup-Vel super-agglomerate displays a much larger spatial distribution complexity. Indeed, the large spread on heliocentric distances, from $\overline{d} = 147\pm6$ pc of IC 2391 to the $d \sim 800$ pc of IC 2395 indicates that not all of them are physically bounded. NGC 2451 A, at $\overline{d} = 181\pm9$ pc, would be another open cluster in the foreground of the extended Vel OB2 association. However, the remaining agglomerates in the super-agglomerate could actually have a common origin. All of them except Pismis 4 ($d \sim 500$–600 pc) lie in a relatively narrow interval of heliocentric distances: (i) vdBH 23 at $\overline{d} = 320\pm30$ pc; (ii) NGC 2451 B at $\overline{d} = 340\pm30$ pc; (iii) Trumpler 10 at $d \sim 360$ pc; (iv) γ Velorum, the core of the Vel OB2 association, NGC 2547, and V468 Pup at $d = 400$–450 pc; and (v) P Puppis at $\overline{d} = 470\pm70$ pc. The mean age of these star clusters is about 30 Ma, with only vdBH 23 having been reported to be significatively younger (age ~ 4 Ma). Although a careful investigation of the parallactic distances to the stars in these agglomerates will not be carried out until the GAIA mission is operative, the resemblance between the ages and distances of γ Velorum and NGC 2547 (that coincide with the trio of agglomerates Escorial 26, 28, and 29) suggests that an important fraction of the Vel OB2 association is actually the superposition of different star-forming regions *à la* Orion.

4.4 Early-type stars at $d \leq 200$ pc

A bit less than 10 % of the investigated OB-type stars are at relatively short heliocentric distances, at $d \leq 200$ pc. Most of them belong to the nearby clusters Pleiades (Escorial 1), NGC 2451 A (Escorial 24), and IC 2391 (Escorial 31), but there are also possible contaminants in the foreground of our agglomerates (listed in last column in Table 1), and errors in the Hipparcos catalogue. On the one hand, cluster stars with accurate parallax measurement are important to derive cluster distances, and compare its spectro-photometric sequence with theoretical models. On the other hand, some of the foreground early-type stars may belong to the rare type of bright B-type dwarfs unbound to known open clusters, which are generally subject of intensive follow-ups in the

literature. Next, we describe the identified early-types stars at $d \leq 200$ pc.

4.4.1 Pleiades

Because of its importance for the "cosmic distance ladder", the disagreement on the actual heliocentric distance to the Pleiades is still an open problem in astrophysics (see recent works by Zwahlen et al. 2004; Soderblom et al. 2005; Southworth, Maxted & Smalley 2005; Percival, Salaris & Groenewegen 2005). Far from taking back again the dispute between the main-sequence fitting and the Hipparcos distance moduli, we have computed an additional measurement of the Pleiades heliocentric distance by weight-averaging the re-reduced Hipparcos parallaxes of the ten stars in our agglomerate Escorial 1. The computed distance to the Pleiades, $\overline{d} = 120\pm5$ pc, is still shorter than the adopted value of 134–139 pc derived from isochrone fitting, but slightly larger than the previous (probably incorrect) Hipparcos distance of 118 pc. The two Hipparcos measurements are, however, consistent with each other within error bars. There is no especial improvement in our $\overline{d}$ if we also add Asterope and Calaeno, classical Pleiads with Hipparcos parallax that were not in our input catalogue (Sect. 3.1.1).

4.4.2 NGC 2451 A

In Sect. 3.4.3, we identified seven Hipparcos stars as members of the NGC 2451 A cluster. Our weight-averaged heliocentric distance to the cluster, $\overline{d} = 181\pm9$ pc, is consistent with (although slightly lower than) the value derived by Robichon et al. (1999) from the original Hipparcos data ($d = 188.7^{+7.0}_{-6.5}$ pc). Carrier et al. (1999) derived, however, $d = 197\pm12$ pc using Geneve photometry and isochrone fitting. Nevertheless, the difference between this value and ours, $\Delta d = 16\pm15$ pc, could be lower if state-of-the-art theoretical tracks and improved metallicity and age were used (as in Platais et al. 2007 for IC 2391 – see below). As a result, there is no hint of NGC 2451 A displaying a Pleiades-like disagreement between heliocentric and isochrone distances.

4.4.3 IC 2391

IC 2391 (Sect. 3.4.2), with an age of about 40 Ma, is probably the youngest open cluster in the solar vicinity (see, however, Barrado y Navascués et al. 2004 and references therein). Platais et al. (2007) have provided the most complete discussion on the problem of the distance to IC 2391. They derived an isochrone distance of 159.2 pc, while the classical Hipparcos distance is $d \sim 146$ pc. From the weight-average of the parallaxes of the seven stars in our Escorial 31 agglomerate, we derive a new Hipparcos distance of $\overline{d} = 147\pm6$ pc. The distance controversy is, therefore, still standing.

Table 2 Early-type field dwarfs at $d \leq 200$ pc.

HIP	Name	Spectral Type	d [pc]	M_V [mag]	$B - V$ [mag]
25469	HD 35716	B9	180±30	2.21	–0.03
25592	HD 35926 AB	B7IV+	180±40	2.08	–0.07
25600	HD 35957	B8	190±40	2.07	–0.05
35083	HD 56342	B3V	193±8	–1.10	–0.14
37173	m Pup A(C)B	B8IV++	190±9	–1.72	–0.09
37229	k^{01} Pup A	B6V	110±8	–0.79	–0.16
	k^{01} Pup B	B5IVn	110±8	–0.58	–0.11
37304	HD 61687 AB	B6V+	193±18	0.34	–0.11
39716	HD 67704	A0V	200±14	0.45	–0.06

4.4.4 Early-type field dwarfs

In Table 2, we list eight foreground agglomerate contaminants at less than $d \leq 200$ pc (one binary was actually resolved by Tycho-2 in its two components). Apart from shorter heliocentric distances than to the corresponding agglomerates, they display different proper motions and, in most cases, are located in abnormal positions in the colour-magnitude diagrams. Six of them are B6–A0 dwarfs at distances $d \approx 180$–200 pc and are not of especial interest. However, the two remaining stars stand out.

As described in Sect. 3.3.2, HD 56342 (B3V, $V_{\rm r}$ = +33.4±2.8 km s^{-1}, $v \sin i$ = 26 km s^{-1}) is a contaminant of the poorly known Collinder 132 cluster. The differences between the HD 56342 and cluster heliocentric distances, $\Delta d \approx 450$ pc, and proper motion, $\Delta \mu \approx 11$ mas a^{-1}, make unlikely its membership in Collinder 132. The star has been spectroscopically investigated in detail by Lyubimkov et al. (2002) and subsequent papers. HD 56342 has typical effective temperature, mass, surface gravity, and helium abundance for its spectral type and class. Furthermore, they derived $d = 209 \pm 36$ pc based solely on spectro-photometric parameters, which is consistent with our parallactic distance ($d = 193 \pm 8$ pc). Savage et al. (1985) and Berghoefer, Schmitt & Cassinelli (1996) also derived independent distances at $d \approx 240$ and 236 pc from ultraviolet interstellar extinction with the Astronomical Netherlands Satellite and from hydrogen column density with ROSAT. With age and mass of 54±9 Ma and 5.3±0.3 M$_\odot$, respectively (Lyubimkov et al. 2002), HD 56342 is one of the very few early B dwarfs in the solar neighbourhood that do not belong to a known cluster.

The case of k^{01} Pup AB (CD–26 4707) is even more extreme. Its proper motion, of $\mu \sim 29$ mas a^{-1}, is inconsistent with membership in the Escorial 23 agglomerate, that probably forms part of the Collinder 121 complex ($d \sim$ 0.5–1.0 kpc). k^{01} Pup AB is a binary system of B5–6 stars (HD 61555 and HD 61556: $\rho = 9.913 \pm 0.003$ arcsec, θ = 318 deg, $\Delta H_P = 0.21 \pm 0.01$ mag; Perryman et al. 1997) located at only $d = 110 \pm 8$ pc. This distance agrees with that estimated by Lindroos (1985), at $d \sim 125$ pc. He also derived a very young age, of about 12 Ma. The evolved nature of the secondary (class IV), that is a helium variable star (Rivinius et al. 2003), may indicate a slightly older

age. In any case, *if* the Hipparcos parallactic distance is correct (binarity may have affected the parallax measurement), k^{01} Pup AB could be the closest massive very young star (age ≤ 50 Ma, $M \geq 5$ M$_\odot$), even closer than the OB-type stars in Upper Scorpius, R Coronae Australis, ρ Ophiuchi, Chamaeleon I+II, and IC 2391 ($d = 130$–150 pc)[13]. We are ignorant of the star-forming region where k^{01} Pup AB was born or if the binary has an associated young moving group.

4.5 Missing agglomerates? Missing stars?

Obviously, our *clustering* algorithm is not able to identify all kinds of star *clusters*, but is mostly sensitive to agglomerates with at least six bright blue stars separated by less than R_ϵ (in our case, $R_\epsilon = 0.8$ deg). Missing cluster types are globular (e.g. ω Cen, M 13) and super star clusters (e.g. Westerlund 1). None of their stellar components were in the input catalogue described in Sect. 2.2 because of their faintness or reddening in the optical $B_{\rm T} V_{\rm T}$ bandpasses (due, in their turn, to very large heliocentric distances, evolution towards the red giant and asymptotic giant branches, or high interstellar extinction).

Some well-known open clusters are also missing. These lacking open clusters can be divided into two classes: (i) clusters with ages in the approximate interval 100–600 Ma (e.g. α Persei, NGC 2516, M 35, Prasepe, Hyades), and (ii) clusters with ages in the approximate interval 1–10 Ma (e.g. Serpens, MBM 12, ρ Ophiuchi, IC 348, λ Orionis, $h + \chi$ Persei). There exist also explanations for their non-detection: for example, there is no Hyades member with Hipparcos colour bluer than $B_{\rm T} - V_{\rm T} = 0.0$ mag. The brightest Hyads, Aldebaran and θ^{02} Tau, are K5III and A7III giants, while the bluest Hyad with reliable Hipparcos photometry, 68 Tau AB, is an A2IV subgiant. In other words, because of stellar evolution, the Hyades turn-off point is redwards of our colour selection criterion in Sect. 2.2. Something similar happens to the other 100–600 Ma open clusters.

In contrast, the effect of the post-main sequence evolution is barely detectable in the 1–10 Ma-old open clusters. However, the early-type stars in the youngest ones (e.g. ρ Ophiuchi, IC 348) also have red colours for their respective spectral types because of intra-cluster extinction (there are abundant populations of Class 0 and I objects – recently born stars surrounded by thick shells – in many of these star-forming regions). The remaining young open clusters with relatively low extinction (e.g. λ Orionis) have looser, less abundant, early-type stellar populations than our 35 agglomerates. Our clustering algorithm is not sensitive, either, to the detection of sparse very young associations, like Taurus-Auriga and TW Hydrae, and low-density Galactic OB associations, like many of those listed in Garmany & Stencel (1992).

---

[13] The most massive nearby star is probably β Pic (A6V, d = 19.27±0.19 pc, age $\sim$ 12 Ma). k^{01} Pup AB, roughly contemporary, would be five times further, but would also be much more massive.

4.6 Effect of the parameterization on the results

We have investigated how a different choice of parameters of the DBSCAN algorithm (in particular, R_ϵ) would have affected our results. On the one hand, Table 3 shows the early-type Hipparcos stars that belong to agglomerates when we use $R_\epsilon = 0.6$ deg instead of 0.8 deg. With the new value, there appear two basic differences: (i) there are only 21 agglomerates, and (ii) the agglomerates contain no more than 11 stars. For example, Escorial 1 (the Pleiades) now contains only six stars, while many other agglomerates, including the young open clusters Collinder 132, M 47, and IC 2395, are not identified at all. Besides, Escorial 3 (25 Ori) is splitted into two different sub-agglomerates (Escorial 3a and 3b), which may indicate the presence of sub-sub-structure in Ori OB1a. Finally, HIP 26727 (Mintaka), that is one of the three bright supergiants in Escorial 6 (Orion Belt), is classified now as a member of Escorial 7 (Horsehead and σ Orionis). To sum up, $R_\epsilon = 0.6$ deg gives an incomplete sampling of our aggregates.

On the other hand, further increasing R_ϵ to 1.0 deg results in the fusion of some aggregates, the detection of some new clusters, and the growth of nearby agglomerates (Fig. 4). In particular:

- 6 agglomerates remain unchanged with respect to the $R_\epsilon = 0.8$ deg parameterization (Escorial 1 [Pleiades], 2 [spurious], 4 [η Ori], 9 [NGC 2264], 27 [vdBH 23], and 32 [IC 2395]).
- 14 agglomerates "capture" nearby bright blue stars and increase in size. Ten of the agglomerates accrete only three or less stars. There are, however, three agglomerates that drastically grow up, capturing 8 (Escorial 3 – 25 Ori), 9 (Escorial 16 – NGC 2232), and up to 12 bright blue stars (Escorial 26 – γ Velorum and NGC 2547).
- 15 agglomerates are fused into five larger entities (with additional capture of nearby bright blue stars). The resultant groupings are the combination of Escorial 6 and 7 (Orion Belt and Horsehead in the Orion super-agglomerate), 10–15 and 17, 18 and 20, 22 and 23 (all agglomerates associated to Collinder 121 along with Collinder 132), and 28 and 29 (in the dense trio in Vel OB2; Sect. 3.4.1). As a result, using $R_\epsilon = 1.0$ deg, the CMa-Pup super-agglomerate is split into only four groupings: Collinder 140 (Escorial 19, the only agglomerate in CMa-Pup that maintain its independence) and the three fusions in Collinder 121. The new Orion division gives the same number of groupings (25 Ori, η Ori, Orion Sword, and "Orion Belt+Horsehead"). Remarkably, the large amassment Escorial 10–15 and 17 contains 135 bright blue stars, a value that does not differ very much from the number of such stars in de Zeeuw et al. (1999)'s Collinder 121 association.
- 19 agglomerates are new. All of them, except three, contain six or seven stars and have surface densities that are $\pi 0.8^2/\pi 1.0^2 = 0.64$ times smaller than our spurious agglomerate Escorial 2. Many of them are probably spurious agglomerates as well, and they would require a

Table 3 Agglomerates of early-type Hipparcos stars with the alternative parameters $N_{\mathrm{MinPts}} = 6$ and $R_\epsilon = 0.6$ deg.

No.	Original Agglomerate (Escorial)	Hipparcos Stars (HIP)
I	1	17499, 17527, 17531, 17573, 17608, 17702
II	2	23279, 23287, 23295, 23328, 23473, 23508
III	3a	25163, 25235, 25288, 25302, 25340, 25469
IV	3b	25241, 25378, 25411, 25533, 25567, 25582, 25592, 25648, 25655, 25751, 25752
V	4	25293, 25394, 25480, 25552, 25557, 25600
VI	5	26197, 26199, 26241, 26314, 26345, 26427
VII	6	26106, 26213, 26311, 26319, 26334, 26405, 26439, 26464, 26508, 26683
VIII	7	26549, 26551, 26579, 26656, 26694, 26713, [26727]
IX	8	30580, 30660, 30700, 30758, 30761, 30772, 30789
X	9	31917, 31951, 31955, 31978, 32030, 32053
XI	10	33062, 33070, 33087, 33165, 33208, 33215, 33276, 33309, 33410
XII	11	33586, 33666, 33695, 33721, 33796, 33841
XIII	12	33935, 33970, 34041, 34048, 34167, 34227
...	13	...
...	14	...
...	15	...
...	16	...
...	17	...
XIV	18	35267, 35370, 35412, 35461, 35503, 35539, 35597
XV	19	35700, 35761, 35795, 35822, 35855, 35905, 36045
...	20	...
...	21	...
...	22	...
...	23	...
...	24	...
XVI	25	37926, 37953, 38020, 38028, 38159, 38164
XVII	26	39873, 39919, 40011, 40016, 40024, 40059
XVIII	27	40218, 40255, 40268, 40274, 40321, 40324
...	28	...
XIX	29	40662, 40742, 40825, 40851, 40872, 40921
...	30	...
XX	31	42400, 42459, 42504, 42535, 42536, 42715, 42726
...	32	...
XXI	33	43055, 43085, 43182, 43209, 42340, 43326, 43392
...	34	...
...	35	...

careful follow-up, as that carried out for the original parameterization. Two of the remaining agglomerates lie on CMa-Pup-Vel region, with $N_\star = 8$ and 9, and may belong to the sparse stellar population of the local spiral arm of the Galaxy (Sect. 3). Finally, there is a new isolated agglomerate with a relative large number of stellar components, $N_\star = 10$, and separated from the large overdensities in Fig. 4. It includes the B0Vp-type star θ Car, that is the brightest one of the IC 2602 open cluster (age ~ 30 Ma, $d = 135\pm9$ pc – Randich et al. 1995; Stauffer et al. 1997).

4.7 Possible errors in the input catalogue

Apart from the large number of Hipparcos stars without parallax determination (indicated with ellipses "..." in the

d column in Table A1), we have also identified two stars that suffered from systematic errors during the Hipparcos reduction. Both of them display proper motions with very large error bars and improbable distances of a few tens AU (indicated with square brackets "[ ]" in the d column in Table A1). They are the binary HIP 23279 + HIP 23287 (HD 32039 + HD 32040, B9Vn, in Escorial 2; $d = 34\pm9$ pc) and HIP 35503 (HD 57281 AB, B5V, in Escorial 18; $d = 70\pm30$ pc). We have not taken them into account in the analysis.

Finally, it seems that there was a misunderstanding in the Bonner Durchmusterung and/or the Hipparcos catalogues between two 10–11th-magnitude stars separated by ∼57 arcsec. The actual K2-type star BD+05 1825 (TYC 189-1314-1), presented in Sect. 2.2, is the easternmost and brightest one of the pair at passbands $V_\mathrm{T} RIJHK_\mathrm{s}$. The westernmost star (HIP 38575, TYC-189-1700-1), that is brighter than BD+05 1825 only at passband B_T, is the only Hipparcos star in the area. HIP 38575 has typical colours of late B or early A dwarfs.

5 Summary

We have used the DBSCAN (Density-Based Spatial Clustering of Applications with Noise) data clustering algorithm to identify spatial agglomerates ("clusters") of Hipparcos stars with colours $B_\mathrm{T} - V_\mathrm{T} < -0.05$ mag.

A total of 35 agglomerates of early-type stars (with spectral types late O, B, and very early A) have arisen from the search. They are ascribed to young open clusters and OB associations, except for a few of them whose physical grouping is uncertain and seem to be spurious detections (Escorial 2 and, possibly, Escorial 16, 30, 34, and 35). Of the remaining agglomerates, four are associated to known open clusters and dense star-forming regions (the Pleiades [Escorial 1], NGC 2264 [Escorial 9], M 47 [Escorial 21], and the poorly known NGC 2232 cluster [Escorial 8]), while 26 form three super-agglomerates (agglomerates of agglomerates).

The Orion super-agglomerate, that coincides with a large fraction of the classical Orion OB1 complex, is splitted into five agglomerates: 25 Orionis (Escorial 3), η Orionis (Escorial 4), Orion Sword (Escorial 5), Orion Belt (Escorial 6), and Horsehead (Escorial 7). This division is atypical: the most important differences with classical divisions are the existence of a new *overdensity* of stars surrounding η Ori AB, and the membership in a population different from the Orion Belt of the σ Orionis cluster. We also confirm the recently identified cluster around 25 Ori.

The CMa-Pup super-agglomerate is broken up into Collinder 132 (Escorial 17), Collinder 140 (Escorial 19), and Collinder 121, which is separated for the first time into ten agglomerates (Escorial 10–15, 18, 20, 22, and 23). The Pup-Vel super-agglomerate is a conglomeration of open clusters in the foreground (at $d < 200$ pc: IC 2391 [Escorial 31], NGC 2451 A [Escorial 24]), background (at $d >$

500 pc: IC 2395 [Escorial 32] and, possibly, Pismis 4 [Escorial 30]), and at the average distance to the Lac OB2 association (at $d = 340$–470 pc). The latter association may comprise different young stellar populations associated to, e.g., Trumpler 10, γ Velorum, and NGC 2547. Many of the agglomerates discussed here need, however, careful spectrophotometric analyses.

The open cluster P Puppis, presented here for the first time, could also be a distant member of the Lac OB2 association. We have carried out a dedicated study of the cluster using Tycho-2, DENIS, and 2MASS data and theoretical isochrones of the Lyon group and quantified its radial density gradient using the normalized cumulative number of cluster member candidates.

We have listed seven agglomerates whose substellar populations will probably be investigated in the future. They are the 25 Orionis and η Orionis overdensities in the Ori OB1a association, the nearby, ∼45 Ma-old cluster NGC 2451 A, and four poorly known clusters at $d = 320$–470 pc with younger ages (NGC 2232, P Puppis, vdBH 23, and Trumpler 10).

We have investigated in detail the early-type Hipparcos stars in agglomerates with heliocentric distances $d \leq 200$ pc. By weight-averaging their parallaxes, we have computed new distances to the Pleiades ($\overline{d} = 120\pm5$ pc), NGC 2451 A ($\overline{d} = 181\pm9$ pc), and IC 2391 ($\overline{d} = 147\pm6$ pc). The dispute between the isochrone fitting and Hipparcos distances still goes on for the Pleiades and IC 2391, but there is no controversial for NGC 2451 A. The remaining ten stars at $d \leq 200$ pc are two stars with errors in the Hipparcos parallax measurements, six B6–A0 dwarfs with typical absolute magnitudes and colours in the foreground, and two standing early/intermediate B stars. The latter stars are HD 56342 (age ∼ 54 Ma, $M \sim 5.3\,\mathrm{M_\odot}$), a B3V star at $d = 193\pm8$ pc, and k^{01} Pup AB, two B5–6 dwarfs separated by $\rho \sim 1090$ AU and located at only $d = 110\pm8$ pc to the Sun. If the Hipparcos parallax measurement is correct, then k^{01} Pup AB would be the closest massive very young star (age ≤ 50 Ma, $M \geq 5\,\mathrm{M_\odot}$).

Finally, we have also discussed which is the effect of the parameter choice (N_MinPts and R_ϵ) on our agglomerate identification and why some known clusters (e.g. Hyades) have not been identified.

Many of the results and hypotheses presented here will be corroborated, refined, or corrected by the future ESA GAIA space mission and subsequent analyses, including more sophisticated data clustering algorithms.

de Strasbourg, France, and the NASA's Astrophysics Data System as bibliographic service. We acknowledge the use of NASA's SkyView facility (http://skyview.gsfc.nasa.gov) located at NASA Goddard Space Flight Center.

References

Adelman, S.J.: 1968, PASP 80, 329

Ambartsumian, V.A.: 1947, *Stellar Evolution and Astrophysics*, Armenian Acad. of Sci., Jerewan

Andersen, T.B., Reiz, A.: 1983, A&AS 53, 181

Asiain, R., Figueras, F., Torra, J., Chen, B.: 1999, A&A 341, 427

Baade, D.: 1982, A&A 105, 65

Baraffe, I., Chabrier, G., Allard, F., Hauschildt, P.H.: 1998, A&A 337, 403

Barbera, M., Bocchino, F., Damiani, F., Micela, G., Sciortino, S., Favata, F., Harnden, F.R., Jr.: 2002, A&A 387, 463

Barrado y Navascués, D., Stauffer, J.R., Jayawardhana, R.: 2004, ApJ 614, 386

Barrow, J.D., Bhavsar, S.P., Sonoda, D.H.: 1985, MNRAS 216, 17

Battinelli, P.: 1991, A&A 244, 69

Battinelli, P., Brandimarti, A., Capuzzo-Dolcetta, R.: 1994, A&AS 104, 379

Battinelli, P., Efremov, Y., Magnier, E.A.: 1996, A&A 314, 51

Baumgardt, H.: 1998, A&A 340, 402

Baumgardt, H., Dettbarn, C., Wielen, R.: 2000, A&AS 146, 251

Bayer, J.: 1603, *Uranometria: Omnium Asterismorum Continens Schemata, Nova Methodo Delineata, Aereis Laminis Expressa*

van den Bergh, S.: 1966, AJ 71, 990

van den Bergh, S., Hagen, G.L.: 1975, AJ 80, 11

Berghoefer, T.W., Schmitt, J.H.M.M., Cassinelli, J.P.: 1996, A&AS 118, 481

Berlind, A.A., Frieman, J., Weinberg, D.H., et al.: 2006, ApJS 167, 1

Bica, E.L.D., Schmitt, H.R.: 1995, ApJS 101, 41

Blaauw, A.: 1964, ARA&A 2, 213

Blaauw, A., Morgan, W.W.: 1953, ApJ 117, 256

Blaha, C., Humphreys, R.M.: 1989, AJ 98, 1598

Boudreault, S., Bailer-Jones, C.A.L.: 2007, AN 328, 709

Briceño, C., Calvet, N., Hernández, J., Vivas, A.K., Hartmann, L., Downes, J.J., Berlind, P.: 2005, AJ 129, 907

Briceño, C., Hartmann, L., Hernández, J., Calvet, N., Vivas, A.K., Furesz, G., Szentgyorgyi, A.: 2007, ApJ 661, 1119

Brown, A.G.A., de Geus, E.J., de Zeeuw, P.T.: 1994, A&A 289, 101

de Bruijne, J.H.J.: 1999, MNRAS 310, 585

Burkert, A., Bate, M.R., Bodenheimer, P.: 1997, MNRAS 289, 497

Caballero, J.A.: 2007, ApJ 667, 520

Caballero, J.A.: 2008a, MNRAS 383, 375

Caballero, J.A.: 2008b, MNRAS 383, 750

Caballero, J.A.: 2008c, A&A 478, 667

Caballero, J.A., Solano, E.: 2008, A&A 485, 931

Caballero, J.A., Burgasser, A.J., Klement, R.: 2008, A&A, in press, arXiv:0805.4480

Carrier, F., Burki, G., Richard, C.: 1999, A&A 341, 469

Chen, B., Asiain, R., Figueras, F., Torra, J.: 1997, A&A 318, 29

Chereul, E., Crézé, M., Bienaymé, O.: 1998, A&A 340, 384

Chereul, E., Crézé, M., Bienaymé, O.: 1998, A&AS 135, 5

Clariá, J.J.: 1972, A&A 19, 303

Clariá, J.J.: 1974, AJ 79, 1022

Clariá, J.J.: 1976, IBVS 1108, 1

Clariá, J.J.: 1977, PASP 89, 803

Clariá, J.J.: 1982, A&AS 47, 323

Clariá, J.J., Rosenzweig, P.: 1978, AJ 83, 278

Clariá, J.J., Lapasset, E., Piatti, A.E., Ahumada, A.V.: 2003, A&A 409, 541

Collinder, P.: 1931, *On Structural Properties of Open Galactic Clusters and Their Spatial Distribution*, Nya Boktryckeriet, Lund

Comerón, F., Torra, J., Gómez, A.E.: 1998, A&A 330, 975

Comerón, F., Torra, J., Jordi, C., Gómez, A.E.: 1993, A&AS 101, 37

Crawford, D.L.: 1961, ApJ, 133, 860

Dahm, S.E., Simon, T.: 2005, AJ 129, 829

Demers, S., Battinelli, P., Irwin, M.J., Kunkel, W.E.: 1995, MNRAS 274, 491

Dias, W.S., Lépine, J.R.D., Alessi, B.S.: 2001, A&A 376, 441

Dias, W.S., Alessi, B.S., Moitinho, A., Lépine, J.R.D.: 2002, A&A 389, 871

Dolidze, M.V.: 1961, Astron. Cir. 223, 11

Dommanget, J., Nys, O.: 1994, Com. de l'Observ. Royal de Belgique 115, 1

Dreyer, J.L.E.: 1888, MmRAS 49, 1

Dutra, C.M., Bica, E., Soares, J., Barbuy, B.: 2003, A&A 400, 533

Eggen, O.J.: 1980, ApJ 238, 627

Eggen, O.J.: 1982, ApJS 50, 199

Eggen, O.J.: 1983, AJ 88, 197

Einasto, J., Klypin, A.A., Saar, E., Shandarin, S.F.: 1984, MNRAS 206, 529

Elmegreen, B.G., Lada, C.J.: 1977, ApJ 214, 725

Epchtein, N., de Batz, B., Capoani, L., et al.: 1997, Messenger 87, 27

Ester, M., Kriegel, H., Sander, J., Xu., X.: 1996, in: E. Simoudis, J. Han, U. Fayyad (eds.), *Knowledge Discovery and Data Mining (KDD'96)*, p. 226

Falin, J.L., Mignard, F.: 1999, A&AS 135, 231

Feigelson, E.D.. Broos, P., Gaffney, J.A., III, Garmire, G., Hillenbrand, L.A., Pravdo, S.H., Townsley, L., Tsuboi, Y.: 2002, ApJ 574, 258

Feinstein, A.: 1966, PASP 78, 301

Feinstein, A.: 1967, ApJ 149, 107

Fernie, J.D.: 1959, MNSSA 18, 57

Fernie, J.D.: 1960, MNSSA 19, 120

Fitzgerald, M.P., Miller, M., Harris, G.L.H.: 1980, MNRAS 191, 95

Fitzgerald, M.P., Harris, G.L., Reed, B.C.: 1990, PASP 102, 865

Flamsteed, J.: 1712, *Historia Coelestis libri Duo quorum prior exhibet Catalogum Stellarum Fixarum Britannicum et Planetarum omnium Observationibus*; posterior Transitus Syderum (...) 1676–1705

Garmany, C.D., Stencel, R.E.: 1992, A&AS 94, 211

Genzel, R., Stutzki, J.: 1989, ARA&A 27, 41

Gilroy, K.K.: 1989, ApJ 347, 835

Gorlova, N., Balog, Z., Rieke, G.H., Muzerolle, J., Su, K.Y.L., Ivanov, V.D., Young, E.T.: 2007, ApJ 670, 516

Gouliermis, D., Kontizas, M., Korakitis, R., Morgan, D.H., Kontizas, E., Dapergolas, A.: 2000, AJ 119, 1737

Griffith, M.R., Wright, A.E.: 1993, AJ 105, 1666

Guetter, H.H.: 1976, AJ 81, 1120

Gum, C.S.: 1955, MmRAS 67, 155

Hardie, R.H., Seyfert, C.K.: 1959, ApJ 129, 601

Harris, G.L.H.: 1976, ApJS 30, 451

Herschel, J.F.W.: 1864, Philosophical Transactions of the Royal Society of London 164, 1

Hillenbrand, L.A.: 1997, AJ 113, 1733

Hiltner, W.A., Garrison, R.F., Schild, R.E.: 1969, ApJ 157, 313

Hoag, A.A., Johnson, H.L., Iriarte, B., Mitchell, R.I., Hallam, K.L., Sharpless, S.: 1961, Publ. U.S. Naval Obs. Second Serie 17, 345

Høg, E., Fabricius, C., Makarov, V.V., et al.: 2000, A&A 355, L27

Hogg, A.R.: 1960, PASP 72, 85

Hoogerwerf, R., Aguilar, L.A.: 1999, MNRAS 306, 394

Hoogerwerf, R., de Bruijne, J.H.J., de Zeeuw, P.T.: 2001, A&A 365, 49

Houk, N.: 1982, *Catalogue of Two-Dimensional Spectral Types for the HD Stars, Vol. 3*, Michigan Spectral Survey, Ann Arbor, Dep. Astron., Univ. Michigan

Huchra, J.P., Geller, M.J.: 1982, ApJ 257, 423

Hünsch, M., Weidner, C., Schmitt, J.H.M.M.: 2003, A&A 402, 571

Hünsch, M., Randich, S., Hempel, M., Weidner, C., Schmitt, J.H.M.M.: 2004, A&A 418, 539

Humphreys, R.M.: 1978, ApJS 38, 309

Irwin, J., Hodgkin, S., Aigrain, S., Bouvier, J., Hebb, L., Moraux, E.: 2008, MNRAS 383, 1588

Ivanov, G.R.: 1996, A&A 305, 708

Jeffries, R.D., Tolley, A.J.: 1998, MNRAS 300, 331

Jeffries, R.D., Oliveira, J.M.: 2005, MNRAS 358, 13

Jeffries, R.D., Totten, E.J., James, D.J.: 2000, MNRAS 316, 950

Jeffries, R.D., Naylor, T., Devey, C.R., Totten, E.J.: 2004, MNRAS 351, 1401

Jeffries, R.D., Evans, P.A., Pye, J.P., Briggs, K.R.: 2006a, MNRAS 367, 781

Jeffries, R.D., Maxted, P.F.L., Oliveira, J.M., Naylor, T.: 2006b, MNRAS 371, L6

Jenkner, H., Maitzen, H.M.: 1987, A&AS 71, 255

Johnson, H.L., Mitchell, R.I.: 1958, ApJ 128, 31

Jørgensen, U.G., Westerlund, B.E.: 1988, A&AS 72, 193

Kaltcheva, N.T., Hilditch, R.W.: 2000, MNRAS 312, 753

Kaltcheva, N.T., Makarov, V.: 2007, ApJ 667, L155

Kaplan, D.L., van Kerkwijk, M.H., Anderson, J.: 2007, ApJ 660, 1428

Kapteyn, J.C.: 1914, ApJ 40, 43

Kharchenko, N.V., Piskunov, A.E., Röser, S., Schilbach, E., Scholz, R.-D.: 2005, A&A 440, 403

Koen, C., Eyer, L.: 2002, MNRAS 331, 45

Koester, D., Reimers, D.: 1985, A&A 153, 260

Kwan, J.: 1977, ApJ 216, 713

de Lacaille, N.L.: 1755, *Nebulae of the Southern Sky*, Observed by M. l'Abbé de la Caille, from the Cape of Good Hope. Mem. Acad. année 1755, page 194 [reprinted in an appendix to: Messier, C. 1780a. Errata important, .., Année 1783. Catalogue des Nébuleuses, page 225. Announce of the discovery of the Messsier objects M69 and M70. Connoissance des Temps for 1783 (published 1780), p. 408]

Lada, C.J., Muench, A. A., Haisch, K. E., Jr., Lada, E. A., Alves, J.F., Tollestrup, E.V., Willner, S.P.: 2000, AJ 120, 3162

Lamm, M.H., Bailer-Jones, C.A.L., Mundt, R., Herbst, W., Scholz, A.: 2004, A&A 417, 557

van Leeuwen, F.: 2007a, Hipparcos, the New Reduction of the Raw Data, Series: Astrophysics and Space Science Library 350, Springer, Dordrecht

van Leeuwen, F.: 2007b, A&A 474, 653

Lesh, J.R.: 1969, AJ 74, 891

Levato, H., Malaroda, S.: 1974, AJ 79, 890

Levato, H., Malaroda, S.: 1975a, PASP 87, 173

Levato, H., Malaroda, S.: 1975b, PASP 87, 823

Levato, H., Abt, H.A.: 1976, PASP 88, 141

Lindroos, K.P.: 1985, A&AS 60, 183

Littlefair, S.P., Naylor, T., Jeffries, R.D., Devey, C.R., Vine, S.: 2003, MNRAS 345, 1205

Lyngå, G.: 1960, ArA 2, 379

Lyngå, G. 1962, ArA 3, 65

Lyngå, G., Wramdemark, S.: 1984, A&A 132, 58

Lyra, W., Moitinho, A., van der Bliek, N.S., Alves, J.: 2006, A&A 453, 101

Lyubimkov, L.S., Rachkovskaya, T.M., Rostopchin, S.I., Lambert, D.L.: 2002, MNRAS 333, 9

Maddox, S.J., Efstathiou, G., Sutherland, W.J., Loveday, J.: 1990, MNRAS 242, 43

Madsen, S., Dravins, D., Lindegren, L.: 2002, A&A 381, 446

Magnier, E.A., Battinelli, P., Lewin, W.H.G., et al.: 1993, A&A 278, 36

Maitzen, H.M., Catalano, F.A.: 1986, A&AS 66, 37

Maíz-Apellániz, J.: 2001, AJ 121, 2737

Martínez, V.J., Jones, B.J.T., Domínguez-Tenreiro, R., van de Weygaert, R.: 1990, ApJ 357, 50

Mel'nik, A.M., Efremov, Yu.N.: 1995, AstL 21, 10

Merchán, M., Zandivarez, A.: 2002, MNRAS 335, 216

Merrill, P.W., Humason, M.L., Burwell, C.G.: 1925, ApJ, 61, 389

Moffat, A.F.J., Vogt, N.: 1975, A&AS 20, 85

Moitinho, A., Alves, J., Huélamo, N., Lada, C.J.: 2001, ApJ 563, L73

Naylor, T., Totten, E.J., Jeffries, R.D., Pozzo, M., Devey, C.R., Thompson, S.A.: 2002, MNRAS 335, 291

Nissen, P.E.: 1988, A&A 199, 146

Oliveira, J.M., Jeffries, R.D., Devey, C.R., Barrado y Navascués, D., Naylor, T., Stauffer, J.R., Totten, E.J.: 2003, MNRAS 342, 651

Otero, S.A., Dubovsky, P.A.: 2004, IBVS 5557, 1

Pallavicini, R., Pasquini, L., Randich, S.: 1992, A&A 261, 245

Pannekoek, A.: 1929, Publ. Astron. Inst. Amsterdam 2, 63

Parenago, P.P.: 1954, Trudy Gosud. Astron. Sternberga 25, 1

Pastoriza, M.G., Ropke, U.O.: 1983, AJ 88, 1769

Patten, B.M., Simon, T.: 1996, ApJS 106, 489

Pedreros, M.H.: 2000, RMxAA 36, 13

Percival, S.M., Salaris, M., Groenewegen, M.A.T.: 2005, A&A 429, 887

Perry, C.L., Hill, G.: 1969, AJ 74, 899

Perryman, M.A.C., Lindegren, L., Kovalevsky, J., et al.: 1997, A&A 323, L49

Pietrzyński, G., Gieren, W., Fouqué, P., Pont, F.: 2001, A&A 371, 497

Piskunov, A.E., Kharchenko, N.V., Röser, S., Schilbach, E., Scholz, R.-D.: 2006, A&A 445, 545

Platais, I., Kozhurina-Platais, V., van Leeuwen, F.: 1998, AJ 116, 2423

Platais, I., Kozhurina-Platais, V., Barnes, S., Girard, T. M.., Demarque, P., van Altena, W.F., Deliyannis, C.P., Horch, E.: 2001, AJ 122, 1486

Platais, I., Melo, C., Mermilliod, J.-C., Kozhurina-Platais, V., Fulbright, J.P., Méndez, R.A., Altmann, M., Sperauskas, J.: 2007, A&A 461, 509

Pols, O.R., Cote, J., Waters, L.B.F.M., Heise, J.: 1991, A&A 241, 419

Press, W.H., Davis, M.: 1982, ApJ 259, 449

Prisinzano, L., Micela, G., Sciortino, S., Favata, F.: 2003, A&A 404, 927

Prosser, C.F., Stauffer, J.R., Hartmann, L., Soderblom, D.R., Jones, B.F., Werner, M.W., McCaughrean, M.J.: 1994, ApJ 421, 517

Randich, S., Schmitt, J.H.M.M., Prosser, C.F., Stauffer, J.R.: 1995, A&A 300, 134

Rebolo, R., Zapatero Osorio, M.R., Martín, E.L.: 1995, Nature 377, 129

Rebull, L.M., Makidon, R.B., Strom, S.E., et al.: 2002, AJ 123, 1528

Reylé, C., Robin, A.C.: 2002, A&A 390, 491

Rivinius, Th., Stahl, O., Baade, D., Kaufer, A.: 2003, IBVS, 5397, 1

Robichon, N., Arenou, F., Mermilliod, J.-C., Turon, C.: 1999, A&A, 345, 471

Rodgers, A.W., Campbell, C.T., Whiteoak, J.B.: 1960, MNRAS, 121, 103

Röser, S., Bastian, U.: 1994, A&A 285, 875

Rojo Arellano, E., Peña, J.H., González, D.: 1997, A&AS 123, 25

Ruprecht, J., Balázs, B., White, R.E.: 1981, *Catalogue of Star Clusters and Associations*, Supplement to Second Edition, Akad. Kiadó, Budapest

Savage, B.D., Massa, D., Meade, M., Wesselius, P.R.: 1985, ApJS 59, 397

Schröder, S.E., Kaper, L., Lamers, H.J.G.L.M., Brown, A.G.A.: 2004, A&A 428, 149

Sharpless, S.: 1952, ApJ 116, 251

Sherry, W.H., Walter, F.M., Wolk, S.J.: 2004, AJ 128, 2316

Shobbrook, R.R.: 1984, MNRAS 211, 659

Siegler, N., Muzerolle, J., Young, E.T., Rieke, G.H., Mamajek, E.E., Trilling, D.E., Gorlova, N., Su, K.Y.L.: 2007, ApJ 654, 580

Skrutskie, M.F., Cutri, R.M., Stiening, R., et al.: 2006, AJ 131, 1163

Skuljan, J., Hearnshaw, J.B., Cottrell, P.L.: 1999, MNRAS 308, 731

Slettebak, A.: 1982, ApJS 50, 55

Smyth, M.J., Nandy, K.: 1962, Publications of the Royal Observatory, Edinburgh 3, 24

Soderblom, D.R., Jones, B.F., Balachandran, S., Stauffer, J.R., Duncan, D.K., Fedele, S.B., Hudon, J.D.: 1993, AJ 106, 1059

Soderblom, D.R., Nelan, E., Benedict, G.F., McArthur, B., Ramírez, I., Spiesman, W., Jones, B.F.: 2005, AJ 129, 1616

Southworth, J., Maxted, P.F.L., Smalley, B.: 2005, A&A 429, 645

Stauffer, J.R., Hartmann, L.W., Jones, B.F., McNamara, B.R.: 1989, ApJ 342, 285

Stauffer, J.R., Caillault, J.-P., Gagne, M., Prosser, C. F., Hartmann, L.W.: 1994, ApJS 91, 625

Stauffer, J.R., Hartmann, L.W., Prosser, C.F., Randich, S., Balachandran, S., Patten, B.M., Simon, T., Giampapa, M.: 1997, ApJ 479, 776

Štefl, S., Baade, D., Rivinius, Th., Otero, S., Stahl, O., Budovičová, A., Kaufer, A., Maintz, M.: 2003, A&A 402, 253

Stift, M.J.: 1979, IBVS 1540, 1

Stock, J.: 1984, RMxAA 9, 127

Strom, S.E., Strom, K.M., Brooke, A.L., Bregman, J., Yost, J.: 1972, ApJ 171, 267

Subramaniam, A., Bhatt, H.C.: 2000, Bulletin of the Astronomical Society of India 28, 255

Tago, E., Einasto, J., Saar, E., Tempel, E., Einasto, M., Vennik, J., Müller, V.: 2008, A&A 479, 927

Turner, E.L., Gott, J.R., III: 1976, ApJS 32, 409

Uchihori, Y., Nagano, M., Takeda, M., Teshima, M., Lloyd-Evans, J., Watson, A.A.: 2000, APh 13, 151

Vandenberg, D.A., Bridges, T.J.: 1984, ApJ 278, 679

Walker, M.F.: 1956, ApJS 2, 365

Walsh, A.J., Hyland, A.R., Robinson, G., Burton, M.G.: 1997, MNRAS 291, 261

Warren, W.H., Jr., Hesser, J.E.: 1977, ApJS 34, 115

Warren, W.H., Jr., Hesser, J.E.: 1978, ApJS 36, 497

Weinmann, S.M., van den Bosch, F.C., Yang, X., Mo, H.J.: 2006, MNRAS 366, 2

Westerlund, B.E.: 1963, MNRAS 127, 71

White, S.D.M., Frenk, C.S.: 1991, ApJ 379, 52

Williams, P.M.: 1966, MNASSA 25, 122

Williams, P.M.: 1967a, MNASSA 26, 126

Williams, P.M.: 1967b, MNASSA 26, 139

Williams, P.M.: 1978, MNRAS 183, 49

Young, E.T., Lada, C.J., Teixeira, P., et al.: 2004, ApJS 154, 428

Young, E.T., Teixeira, P.S., Lada, C.J., et al.: 2006, ApJ 642, 972

de Zeeuw, P.T., Hoogerwerf, R., de Bruijne, J.H.J., Brown, A.G.A., Blaauw, A.: 1999, AJ 117, 354

Zug, R.S.: 1933, Lick Observatory bulletin 16, 119

Zwahlen, N., North, P., Debernardi, Y., Eyer, L., Galland, F., Groenewegen, M.A.T., Hummel, C.A.: 2004, A&A 425, L45

A   Early-type Hipparcos stars in agglomerates

Fig. A1 (online colour at: www.an-journal.org) False-colour DSS-2 images of the agglomerates of early-type *Hipparcos* stars centred on reference stars in Table 1. Blue, green, and red are for photographic B_J, R_F, and I_N. North is up, east is left. All the images are $3 \times 3 \deg^2$ in size. Fits images were obtained from SkyView and combined with DS9. *From left to right*: Escorial 1 (Pleiades), 2, and 3 (25 Ori).

Fig. A2 (online colour at: www.an-journal.org) Same as Fig. A1, but for Escorial 4 (η Ori; *left*), Escorial 5 (Orion Sword; *centre*) and Escorial 6 (Orion Belt; *right*).

Fig. A3 (online colour at: www.an-journal.org) Same as Fig. A1, but for the agglomerates Escorial 7 (Horsehead; *left*), Escorial 8 (NGC 2232; *centre*), and Escorial 9 (NGC 2264; *right*).

Fig. A4 (online colour at: www.an-journal.org) Same as Fig. A1, but for the agglomerates Escorial 10, 11, and 12, from left to right. They are associated to Collinder 121.

Fig. A5 (online colour at: www.an-journal.org) Same as Fig. A1, but for the agglomerates Escorial 13, 14, and 15, from left to right. They are also associated to Collinder 121.

Fig. A6 (online colour at: www.an-journal.org) Same as Fig. A1, but for the agglomerates Escorial 16 (including NGC 2353; *left*), Escorial 17 (Collinder 132; *centre*), and Escorial 18 (associated to Collinder 121; *right*).

Fig. A7 (online colour at: www.an-journal.org) Same as Fig. A1, but for the agglomerates Escorial 19 (Collinder 140; *left*), Escorial 20 (associated to Collinder 121; *centre*), and Escorial 21 (M 47; *right*).

Fig. A8 (online colour at: www.an-journal.org) Same as Fig. A1, but for the agglomerates Escorial 22 and 23 (associated to Collinder 121) and Escorial 24 (NGC 2451 AB; *right*).

Fig. A9 (online colour at: www.an-journal.org) Same as Fig. A1, but for the agglomerates Escorial 25 (P Puppis; *left*), Escorial 26 (associated to Vel OB2, and including NGC 2547 and γ Velorum; *centre*), and Escorial 27 (vdBH 23; *right*).

Fig. A10 (online colour at: www.an-journal.org) Same as Fig. A1, but for the agglomerates Escorial 28 and 29 (associated to Vel OB2), and Escorial 30 (including vdBH 34 and Pismis 4; *right*).
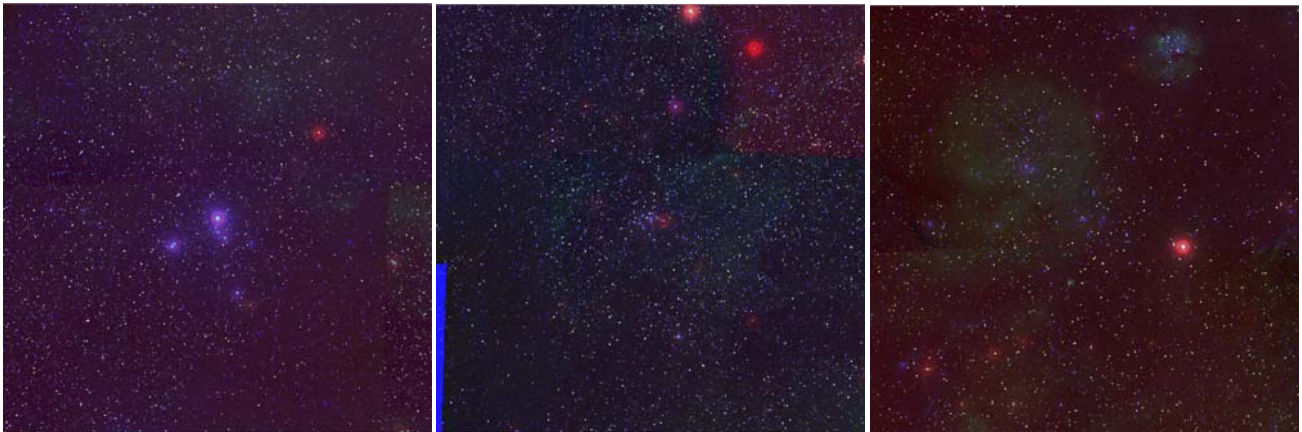
Fig. A11 (online colour at: www.an-journal.org) Same as Fig. A1, but for the agglomerates Escorial 31 (IC 2391; *left*), Escorial 32 (IC 2395; *centre*), and Escorial 33 (Trumpler 10; *right*).

Fig. A12 (online colour at: www.an-journal.org) Same as Fig. A1, but for the agglomerates Escorial 34 and 35.

Table A1: Early-type Hipparcos stars in aggregates.

Agglomerate	HIP	Name	Spectral Type	d [pc]	α (J2000)	δ (J2000)	$\mu_\alpha \cos\delta$ [mas a^{-1}]	μ_δ [mas a^{-1}]
Escorial 1	17499	Electra	B6IIIe	124±4	03 44 52.54	+24 06 48.0	+20.9±0.3	−46.0±0.2
	17527	18 Tau	B8V	125±6	03 45 09.74	+24 50 21.3	+20.4±0.4	−46.5±0.4
	17531	Taygeta	B6IV	125±5	03 45 12.49	+24 28 02.2	+21.3±0.4	−40.5±0.4
	17573	Maia	B8III	117±4	03 45 49.61	+24 22 03.9	+21.2±0.4	−46.0±0.3
	17608	Merope	B6IVe	116±5	03 46 19.57	+23 56 54.1	+21.2±0.4	−43.6±0.3
	17702	Alcyone	B7IIIe	124±6	03 47 29.08	+24 06 18.5	+19.3±0.4	−43.7±0.3
	17776	HD 23753	B8V	118±5	03 48 20.82	+23 25 16.5	+18.0±0.4	−46.6±0.3
	17847	Atlas AB	B8III+	117±5	03 49 09.74	+24 03 12.3	+17.7±0.4	−44.2±0.3
	17851	Pleione	B8IVev	117±4	03 49 11.22	+24 08 12.2	+18.1±0.3	−47.2±0.3
	17900	HD 23923	B8V	115±8	03 49 43.53	+23 42 42.7	+16.7±0.6	−44.8±0.5
Escorial 2	23279	HD 32039	B9Vn	...	05 00 32.54	+03 36 53.3	(+10.5±1.3)	(−18.2±1.3)
	23287	HD 32040	B9Vn	[34±9]	05 00 33.93	+03 36 56.7	(+13.0±1.4)	(−16.1±1.3)
	23295	HD 32056	B9	220±70	05 00 39.79	+03 15 55.2	+0.4±1.3	−4.6±0.8
	23328	V1360 Ori	B8V	260±40	05 01 06.02	+03 43 02.4	−2.0±0.7	−6.7±0.4
	23473	HD 32359	B9V	500±200	05 02 44.55	+03 27 27.7	+2.5±0.8	−3.8±0.6
	23508	HD 32431	B8V	...	05 03 17.10	+04 00 56.0	+0.5±1.0	+3.8±0.7
Escorial 3	25163	HD 35177	B9	350±150	05 23 01.93	+01 41 48.9	−1.0±1.2	−1.1±0.6
	25164	HD 35194	B9	270±70	05 23 01.96	+00 26 20.6	−1.3±0.9	−3.0±0.6
	25179	HD 35203	B6V	320±90	05 23 10.15	+01 08 22.6	−2.7±1.0	−3.2±0.5
	25235	V1156 Ori	B3Vw	...	05 23 50.36	+02 04 55.8	+0.4±1.0	+0.9±0.5
	25241	HD 35305	B6.5IV/V	380±130	05 23 51.38	+00 51 46.3	+3.1±0.9	−0.8±0.5
	25288	HD 35407	B4IVn	470±160	05 24 36.10	+02 21 11.4	−0.2±0.7	−0.9±0.4
	25302	25 Ori	B1Vpe	320±90	05 24 44.83	+01 50 47.2	+0.2±0.7	−0.2±0.4
	25340	HD 35501 AB	B8V+	...	05 25 11.40	+01 55 24.0	+1.0±1.1	−2.9±0.5
	25378	HD 35588 AB	B2.5V+	380±60	05 25 47.02	+00 31 12.9	+1.2±0.4	−0.8±0.2
	25411	HD 35612	B8	320±100	05 26 06.00	+00 50 02.4	+2.0±0.9	−1.8±0.5
	25469	HD 35716	B9	180±30	05 26 48.11	+02 04 05.9	−2.3±1.1	+0.1±0.5
	25533	HD 35834 AB	B8V+	370±150	05 27 36.88	+01 06 27.3	−0.2±1.1	+2.1±0.5
	25567	HD 35881	B8V	210±50	05 27 54.23	+01 06 18.2	+1.0±1.0	−0.2±0.5
	25582	HD 35912	B2V	400±90	05 28 01.47	+01 17 53.7	−0.9±0.6	+0.7±0.3
	25592	HD 35926 AB	B7IV+	180±40	05 28 10.12	+00 47 14.0	−1.7±1.3	−3.2±0.6
	25648	HD 36013	B3V:n	320±60	05 28 45.29	+01 38 38.2	−1.0±0.6	−0.2±0.3
	25655	V1372 Ori	B5Vne	390±90	05 28 48.46	+02 09 53.0	−1.7±0.5	−0.6±0.3
	25751	HD 36166	B2V	440±70	05 29 54.77	+01 47 21.3	+1.3±0.4	−1.33±0.18
	25752	HD 36165	B7V	230±50	05 29 55.55	+02 08 31.8	−2.0±0.8	+0.4±0.4
	25881	HD 36392	B3V	250±60	05 31 29.89	+01 41 24.1	−1.9±1.2	+0.1±0.5
	25897	HD 36429	B5V	200±30	05 31 41.22	+02 49 58.2	+2.6±0.8	−1.3±0.4
	25979	HD 36549	B6Vwp	320±130	05 32 39.49	+02 05 31.8	+3.5±1.3	−0.9±0.5
	26098	HD 36741	B2V	340±60	05 33 57.59	+01 24 27.5	+2.8±0.6	−0.6±0.2
Escorial 4	25281	η Ori AB	B0.5V+	310±100	05 24 28.62	−02 23 49.7	−0.8±1.1	−3.6±0.8
	25293	HD 35456 AB	B8V+	600±200	05 24 40.38	−02 29 52.3	−3.6±0.7	−1.9±0.4
	25368	HD 35575	B3V	230±20	05 25 36.50	−01 29 28.7	+3.6±0.4	−0.7±0.2
	25394	V1370 Ori	B8	410±160	05 25 55.87	−02 20 07.9	+1.4±0.9	−2.5±0.6
	25480	HD 35777	B2V	300±80	05 26 59.16	−02 21 38.3	+1.7±0.6	−2.0±0.3
	25496	HD 35792	B3V	240±30	05 27 09.37	−02 20 07.9	+1.5±0.6	−3.0±0.4
	25552	HD 35882	B8	400±110	05 27 44.72	−01 22 02.5	+2.0±0.6	−2.0±0.4
	25557	HD 35899	B5V	340±80	05 27 45.77	−02 08 43.7	+2.9±0.6	−1.8±0.4
	25600	HD 35957	B8	190±40	05 28 12.63	−01 56 28.5	+1.1±1.1	−0.9±0.7
Escorial 5	25712	HD 36151	B5V	470±100	05 29 25.41	−07 15 39.2	+0.6±0.4	−1.8±0.3
	25786	HD 36285	B2IV/V	700±200	05 30 20.75	−07 26 05.3	+1.4±0.4	−1.0±0.3
	25869	HD 36430	B2V	710±180	05 31 20.89	−06 42 30.2	+1.3±0.3	+0.5±0.2
	25898	HD 36487	B5V	700±300	05 31 41.44	−07 02 55.1	+0.8±0.6	−0.1±0.5
	25923	υ Ori	B0V	880±190	05 31 55.86	−07 18 05.5	−0.10±0.18	−4.87±0.14
	25937	HD 36541	B8V	800±300	05 32 07.03	−06 42 29.9	+0.3±0.5	+0.1±0.4
	25962	HD 36560	A0	300±90	05 32 18.92	−06 23 33.1	+1.1±0.8	−1.1±0.6
	26182	V1045 Ori	B8IIIp	270±50	05 34 53.96	−04 06 37.5	−5.7±0.6	−0.8±0.4
	26197	HD 36959	B1Vv	800±300	05 35 01.01	−06 00 33.4	+0.5±0.4	−1.5±0.2
	26199	HD 36960	B0.5V	500±80	05 35 02.68	−06 00 07.3	−0.7±0.3	+0.01±0.19
	26233	V1046 Ori	B1.5V	380±110	05 35 21.87	−04 29 39.0	+1.3±0.6	+0.5±0.4
	26234	HD 37016 AB	B2.5V+	410±140	05 35 22.32	−04 25 27.6	−0.1±0.7	+0.8±0.4
	26237	c Ori AB	B1V+	270±90	05 35 23.16	−04 50 18.1	+4.5±1.1	−7.1±0.7
	26241	ι Ori AC	O9III+	710±110	05 35 25.98	−05 54 35.6	+1.4±0.2	−0.47±0.13
	26257	HD 37040 AB	B2.5IV+	350±100	05 35 31.08	−04 21 50.6	+4.2±0.7	−0.2±0.5
	26314	HD 37150	B3Vv	390±100	05 36 16.03	−05 38 52.5	+0.6±0.6	−1.3±0.4
	26345	HD 37209	B1V	470±100	05 36 35.69	−06 03 53.1	−0.2±0.4	+0.1±0.2
	26427	HD 37303	B1Vv	410±80	05 37 27.36	−05 56 18.2	+1.8±0.4	−2.1±0.3
	26442	V1378 Ori	B1.5V	430±120	05 37 36.75	−04 56 02.8	+0.6±0.7	+3.4±0.4
	26477	HD 37356	B2IV/V	490±110	05 37 53.39	−04 48 50.5	−1.7±0.5	+0.9±0.3
	26535	HD 37481	B1.5IV	410±70	05 38 37.97	−06 34 26.3	+0.6±0.3	−0.2±0.2
	26581	HD 37526	B3V	400±100	05 39 02.40	−05 11 40.1	+1.4±0.6	−4.4±0.3
	26697	HD 37700	B6V	700±400	05 40 25.25	−04 25 16.4	+1.9±0.7	+0.8±0.4
Escorial 6	25930	Mintaka AE–D	O9.5II++	210±30	05 32 00.40	−00 17 56.7	+0.6±0.6	−0.7±0.3
	25980	HD 36591 AB	B1IV+	480±180	05 32 41.35	−01 35 30.6	−2.0±0.7	+0.8±0.4
	26020	HD 36646 AB	B4Vn+	320±70	05 33 07.35	−01 43 02.5	+0.2±0.6	+0.4±0.4
	26048	V1107 Ori	B6Vwp	250±40	05 33 26.06	+00 37 16.9	+0.3±0.8	−1.1±0.4
	26063	VV Ori AB	B1.0V+	450±70	05 33 31.45	−01 09 21.9	−0.8±0.3	−1.07±0.18
	26082	HD 36709	A0	260±50	05 33 45.45	−00 01 44.1	−2.0±1.0	+1.1±0.5
	26106	HD 36779 AC	B2.5V	310±40	05 34 03.89	−01 02 08.6	+2.7±0.4	−3.2±0.2
	26188	HD 36898	B5	230±40	05 34 56.49	−00 07 22.3	−2.9±0.8	−5.5±0.4

Continued on next page.

Table A1: Continued.

Agglomerate	HIP	Name	Spectral type	d [pc]	α (J2000)	δ (J2000)	$\mu_\alpha \cos \delta$ [mas a^{-1}]	μ_δ [mas a^{-1}]
	26210	HD 36935	B7V	330±80	05 35 09.21	−00 16 10.6	+1.5±0.7	−0.2±0.3
	26213	HD 36954 AB	B3V+	340±70	05 35 12.79	−00 44 07.3	+0.3±0.6	+1.5±0.3
	26311	Alnilam A	B0Iab:	610±160	05 36 12.81	−01 12 06.9	+1.5±0.4	−0.78±0.19
	26319	HD 37149	B8Ve	400±120	05 36 17.83	−01 38 07.2	+1.2±0.8	−0.2±0.4
	26334	HD 37173	B6V	...	05 36 30.59	−01 59 01.8	−0.8±0.9	+3.4±0.5
	26405	HD 37272	B5V	(500±200)	05 37 14.52	−01 40 03.8	+0.5±1.0	−1.0±0.5
	26431	HD 37294	A0	...	05 37 30.30	−00 14 25.5	−3.3±1.1	−1.0±0.5
	26439	HD 37321 AB	B4V+	(400±170)	05 37 34.80	−01 25 19.7	+0.8±1.0	−1.2±0.5
	26464	V1379 Ori	B5V	270±50	05 37 45.89	−00 46 41.7	+0.8±0.8	−2.3±0.3
	26508	HD 37397	B2V	470±140	05 38 13.74	−01 10 09.0	+0.8±0.7	−1.5±0.3
	26526	HD 37427	B8V	...	05 38 31.33	−00 08 52.0	−3.3±1.3	−0.8±0.6
	26683	HD 37674	B3Vn	310±80	05 40 13.54	−01 27 45.2	−0.6±0.9	+2.0±0.4
	26727	Alnitak AB	O9.5Ib+	230±30	05 40 45.53	−01 56 33.3	+3.1±0.6	+2.1±0.3
	26736	HD 37756 AB	B2IV/V+	270±50	05 40 50.71	−01 07 43.6	−1.5±0.4	−0.84±0.19
	26742	V901 Ori	B2IV	330±60	05 40 56.37	−01 30 25.9	+3.2±0.7	+1.8±0.3
Escorial 7	26549	σ Ori AF–B	O9.5V++	(350±100)	05 38 44.77	−02 36 00.2	(+4.6±0.9)	(−0.4±0.5)
	26551	σ Ori D	B2V	210±30	05 38 45.63	−02 35 58.9	+0.6±0.7	−0.8±0.4
	26579	HD 37525 AB	B5V+	310±90	05 39 01.49	−02 38 56.4	−1.2±0.9	−0.9±0.4
	26656	V1148 Ori	B9	...	05 39 55.42	−03 19 49.8	+2.3±0.7	−1.3±0.4
	26694	HD 37699	B5V	...	05 40 20.19	−02 26 08.2	+1.5±0.8	−0.2±0.3
	26713	HD 37744	B1.5V	410±80	05 40 37.30	−02 49 30.9	+1.6±0.4	+2.1±0.2
	26766	HD 37807	B8	...	05 41 08.13	−03 37 57.2	+1.8±0.8	−2.4±0.4
Escorial 8	30580	HD 45153	B8	210±30	06 25 38.92	−04 49 56.3	−8.9±0.7	−5.0±0.5
	30660	HD 45321	B2.5V	400±80	06 26 34.44	−04 35 50.6	−4.3±0.5	−1.7±0.4
	30700	9 Mon	B5	300±40	06 27 00.88	−04 21 20.4	−5.8±0.5	−3.7±0.4
	30758	HD 45516	B9	340±80	06 27 47.62	−04 49 29.0	−5.8±0.7	−1.6±0.6
	30761	HD 45532	A0	330±70	06 27 50.84	−05 09 17.5	−4.8±0.6	−4.0±0.5
	30772	10 Mon	B2V	330±30	06 27 57.57	−04 45 43.8	−5.8±0.2	−2.85±0.18
	30789	V682 Mon	B8	290±70	06 28 10.77	−04 53 56.5	−6.5±0.8	−1.1±0.7
	31011	HD 45975	B9	200±20	06 30 27.47	−04 41 48.5	−9.0±0.5	−0.7±0.5
	31101	HD 46165	B9	310±50	06 31 36.09	−05 22 07.4	−4.9±0.4	−1.4±0.4
Escorial 9	31917	HD 47662	B7V	500±200	06 40 13.37	+10 26 28.7	−2.6±1.0	−0.9±0.7
	31951	HD 47754	B9V	(380±170)	06 40 36.53	+10 23 31.0	−3.0±1.2	−2.8±0.8
	31955	HD 47777	B3V	...	06 40 42.29	+09 39 21.3	−2.0±1.0	−4.4±0.6
	31978	S Mon AB	O7Ve+	280±40	06 40 58.66	+09 53 44.7	−2.6±0.6	−1.6±0.4
	32030	HD 47961	B2V	450±140	06 41 27.30	+09 51 14.4	−3.2±0.8	−2.8±0.5
	32053	HD 48055	B9V	260±80	06 41 49.71	+09 30 29.4	−2.5±1.6	−3.1±1.0
Escorial 10	32561	HD 49485	B8II	500±200	06 47 39.18	−24 56 36.2	−4.6±0.4	−6.1±0.6
	32823	HD 50074	B5V	...	06 50 32.66	−24 57 32.7	−2.0±0.7	+4.2±1.0
	32827	HD 50093	B2III/IV	480±90	06 50 36.96	−25 46 42.2	−4.2±0.2	+5.6±0.4
	32861	HD 50155	B8–9V	...	06 50 55.92	−24 44 16.4	−1.3±0.6	−3.6±0.8
	32867	HD 50154	B2–3Vn	...	06 50 58.09	−24 23 53.8	−1.9±0.6	+5.5±0.8
	32882	HD 50176	B7–8III/IV	300±150	06 51 06.29	−24 42 22.6	−1.7±1.0	+5.2±1.3
	32911	HD 50261	B8IV/V	290±70	06 51 26.42	−25 22 09.6	−2.1±0.5	+4.3±0.7
	33019	HD 50535	B8V	480±170	06 52 47.60	−23 02 49.3	−2.6±0.5	+6.9±0.7
	33057	HD 50647	B5V	...	06 53 07.99	−24 54 27.3	−2.8±0.6	+4.2±0.9
	33062	HD 50646	B2II/III	...	06 53 12.91	−24 10 00.0	−2.2±0.4	+5.3±0.6
	33070	HD 50680	B3II/III	(400±200)	06 53 15.45	−24 06 59.6	−2.9±0.4	+4.7±0.7
	33087	HD 50740	B9V	...	06 53 27.58	−24 06 42.5	−6.1±0.6	−1.3±1.0
	33165	EZ CMa	WN4	(600±300)	06 54 13.04	−23 55 42.0	−3.8±0.3	+4.3±0.6
	33182	HD 50939	B2–3V	380±140	06 54 22.49	−23 02 52.2	−3.0±0.7	+3.0±0.8
	33208	HD 51013	B3V	...	06 54 41.21	−24 15 20.4	−2.9±0.5	+3.9±0.8
	33211	HD 51038	B3V	330±100	06 54 42.58	−24 55 28.8	−3.4±0.6	+2.0±0.9
	33215	HD 51036	B6–7	...	06 54 44.64	−24 18 57.8	−2.8±0.6	+3.8±0.9
	33276	HD 51155	B6V	...	06 55 18.22	−23 32 16.6	−1.3±0.7	+5.9±1.0
	33309	HD 51285	B2Ve	...	06 55 42.84	−24 40 43.8	−4.8±0.5	+3.9±0.7
	33316	HD 51283	B2–3III	(700±300)	06 55 46.93	−22 56 29.2	−2.6±0.2	+3.3±0.3
	33410	HD 51575	B8II/III	290±120	06 56 53.99	−24 30 51.1	−10.2±1.5	+2.5±1.3
Escorial 11	33246	HD 51056	A2III	...	06 55 02.14	−20 40 27.5	−1.8±0.9	+3.1±1.2
	33260	LM CMa	B9Ib/II	...	06 55 11.74	−21 52 18.9	−4.6±0.6	+2.8±0.9
	33294	HD 51200	B2III/IV	(700±300)	06 55 32.89	−22 02 14.8	−3.6±0.4	+2.2±0.4
	33343	HD 51340 AB	B5V+	320±120	06 56 04.34	−21 30 21.3	−2.4±0.7	+2.3±1.1
	33412	HD 51549	B3IV	...	06 56 55.27	−21 06 04.9	−2.0±0.4	+2.9±0.6
	33447	HH CMa	B2III/IV	550±140	06 57 14.77	−22 12 10.3	−1.4±0.4	+2.7±0.5
	33504	HD 51790	Ap	280±100	06 57 51.16	−21 56 14.0	−5.1±0.8	+3.8±1.1
	33522	HD 51819	B6V	...	06 58 01.26	−20 58 00.6	−2.9±0.7	+3.2±0.9
	33523	HD 51854	B2V	...	06 58 02.12	−22 52 34.0	−3.6±0.8	+4.6±0.9
	33554	HD 51898	B2–3V	...	06 58 12.92	−20 31 46.3	−2.1±0.6	+3.1±0.7
	33586	HD 51984	B5III	...	06 58 39.02	−22 32 10.0	−2.3±1.0	+2.5±1.2
	33621	HD 52115	B8II/III	...	06 59 07.18	−20 47 32.0	−3.9±0.4	+3.8±0.6
	33635	HD 52165 AB	B3V+	...	06 59 14.59	−21 22 46.8	−2.7±1.1	+5.5±1.9
	33666	HD 52273	B2III	390±70	06 59 39.25	−21 36 10.4	−2.9±0.2	+4.3±0.3
	33695	HD 52349	B5IV	310±120	07 00 03.90	−21 48 16.7	−4.2±0.8	+2.8±1.0
	33703	HD 52348	B3V	430±90	07 00 08.28	−20 09 30.3	−5.5±0.4	+6.5±0.4
	33721	FU CMa AP	B3Vnne+	600±200	07 00 19.36	−22 07 08.6	−2.8±0.3	+3.4±0.4
	33796	HD 52614	B5V	360±170	07 01 02.93	−22 31 28.8	−2.8±1.0	+2.6±1.0
	33841	BD–22 1661	B5	...	07 01 30.17	−22 33 45.8	−2.9±1.0	+3.7±1.2
Escorial 12	33532	HD 51925 AB	B2.5III+	800±300	06 58 07.55	−27 09 51.8	−2.9±0.3	+3.3±0.4
	33575	HD 52018	B2V	260±20	06 58 35.90	−25 24 51.0	−6.49±0.17	+5.2±0.3

Continued on next page.

Table A1: Continued.

Agglomerate	HIP	Name	Spectral type	d [pc]	α (J2000)	δ (J2000)	$\mu_\alpha \cos\delta$ [mas a^{-1}]	μ_δ [mas a^{-1}]
	33611	HD 52138 AB	B2V+	430±110	06 59 00.59	−26 28 27.9	−2.6±0.3	+3.2±0.6
	33708	HD 52463	B3V	...	07 00 12.27	−27 47 59.8	−3.3±0.6	+3.1±0.8
	33745	HD 52511	B5IV/V	280±90	07 00 36.18	−23 51 19.4	−1.0±0.8	+2.6±1.1
	33769	HD 52597	B2–3Ve	...	07 00 47.54	−26 05 36.4	−2.6±0.4	+4.0±0.6
	33770	HD 52596 AB	B2IV+	520±160	07 00 47.55	−25 38 37.7	−3.1±0.4	+2.7±0.5
	33775	HD 52616	B7–8V	300±80	07 00 50.68	−26 57 34.7	−1.3±0.6	+1.3±0.8
	33778	LR CMa	B9II	...	07 00 51.15	−23 35 47.8	−1.9±0.7	+2.8±0.8
	33804	LS CMa	B2–3III/IV	310±30	07 01 05.95	−25 12 56.3	−4.78±0.17	+4.5±0.3
	33814	HD 52731	B3V	380±110	07 01 12.23	−27 41 14.7	−2.4±0.5	+2.7±0.7
	33828	HD 52726	B7–8V	...	07 01 21.62	−25 12 21.8	−4.0±0.7	+6.3±1.2
	33846	HD 52812	B3Ve	700±200	07 01 33.61	−27 13 22.6	−3.2±0.4	+3.8±0.5
	33865	HD 52849	B3IV	...	07 01 47.79	−23 27 32.6	−4.4±0.6	+4.0±0.8
	33882	HD 52928	B8IV/V	...	07 01 57.88	−26 16 33.3	−4.1±0.7	+3.9±1.0
	33888	HD 52945	B9V(+)	...	07 02 03.50	−26 34 04.3	−2.8±0.7	+2.3±0.9
	33924	HD 53040	B8	...	07 02 23.04	−26 45 01.0	−1.7±1.0	+5.5±1.4
	33935	HD 53019	A0V	290±120	07 02 29.08	−24 52 36.6	−2.2±0.8	+2.0±0.9
	33970	HD 53123	B9V	270±40	07 02 54.56	−24 34 59.2	−4.8±0.3	+13.0±0.5
	33977	24 CMa	B3Ia	800±300	07 03 01.47	−23 49 59.8	−2.2±0.4	+3.6±0.4
	34041	HD 53344	B2–3V	510±110	07 03 42.91	−25 05 02.1	−3.4±0.2	+3.2±0.4
	34044	HD 53342	B8V	...	07 03 44.91	−24 18 39.1	−5.0±0.5	+3.7±1.0
	34048	HD 53373	B2III/IV	500±150	07 03 47.42	−25 39 12.2	−2.5±0.4	+2.4±0.6
	34067	HD 53461	B3III	580±190	07 03 58.04	−27 30 20.3	−3.9±0.4	+5.0±0.5
	34139	HD 53654	B5V	...	07 04 44.53	−27 08 52.6	−2.2±0.7	+2.0±0.9
	34153	HD 53673	B8V	500±200	07 04 54.18	−26 36 38.8	−3.6±0.6	+4.2±0.9
	34167	HD 53728	B2IV	600±300	07 05 06.95	−25 06 02.0	−3.7±0.3	+2.8±0.7
	34220	HD 53914	B4IV	...	07 05 41.61	−27 17 44.0	−4.7±0.6	+1.8±0.7
	34227	HD 53885	B3V:n	...	07 05 46.05	−25 00 28.2	−2.6±0.4	+5.1±0.9
	34281	HD 54063	B5V	...	07 06 27.35	−25 28 11.6	−3.5±0.5	+4.2±0.9
	34331	HD 54224	B2IV/V	700±200	07 06 59.99	−26 39 24.3	−3.9±0.2	+4.0±0.3
	34371	HD 54337	B8–9V	500±200	07 07 27.88	−25 36 12.6	−1.5±0.4	+4.6±0.7
Escorial 13	34360	FV CMa	B2V:nne	...	07 07 22.59	−23 50 26.6	−3.4±0.5	+6.1±0.6
	34429	HD 54551	B1–2II	...	07 08 14.79	−23 25 54.1	−2.1±0.7	+2.9±1.0
	34455	HD 54604	B9III	...	07 08 32.39	−23 09 32.5	+2.1±0.8	−2.1±1.1
	34478	HD 54641	B3V	...	07 08 44.46	−23 46 30.5	−5.0±0.6	+1.8±0.8
	34489	HD 54669	B4V	...	07 08 49.40	−24 02 37.6	−2.5±0.4	+3.4±0.5
	34599	HD 54962 AB	Ap+	...	07 09 58.40	−24 24 35.2	−4.5±0.9	−0.2±1.2
	34637	HD 55040	B8V	...	07 10 26.54	−24 20 46.5	−4.4±0.6	+2.0±0.8
Escorial 14	34251	HD 54006	B8–9III/IV	...	07 06 01.61	−28 19 16.6	−3.7±0.9	+3.0±1.1
	34412	HD 54555	B3IV	...	07 08 03.02	−28 34 36.7	−3.4±0.6	+1.1±0.7
	34507	HD 54771 AB	B3IV+	...	07 09 00.59	−28 09 32.9	−3.1±0.4	+3.5±0.6
	34528	HD 54816	B8–9III	300±80	07 09 15.42	−27 21 46.1	−3.8±0.6	+6.3±0.8
	34562	HD 54913	B2V	...	07 09 33.32	−28 26 40.6	−2.6±0.5	+3.6±0.7
	34601	HD 55019	B2V	580±180	07 10 00.52	−28 44 53.4	−4.1±0.3	+3.7±0.5
Escorial 15	34781	CD–27 3748	B5p	...	07 12 02.29	−27 43 04.9	−5.2±0.8	−0.3±1.0
	34786	HD 55523	B3III	370±70	07 12 05.39	−27 20 05.8	−9.3±0.3	+4.3±0.4
	34798	MM CMa	B2IV/V	260±30	07 12 12.21	−25 56 33.3	−5.5±0.2	+7.9±0.3
	34871	CD–27 4012	B9	...	07 12 55.49	−28 13 19.7	−5.0±0.8	+3.5±1.1
	34924	GY CMa	B0.5V	1100±500	07 13 36.45	−27 21 22.9	−3.9±0.3	+6.4±0.4
	34948	HD 55906	B3III	...	07 13 53.13	−27 17 40.2	−3.6±0.7	+3.2±0.8
	34981	27 CMa AB	B3IIIe+	530±90	07 14 15.21	−26 21 09.0	−6.91±0.18	+3.2±0.3
	34983	HD 56044	B3V	600±200	07 14 16.79	−28 10 10.3	−4.0±0.4	+4.1±0.7
	35037	ω CMa	B2IV/Ve	279±13	07 14 48.65	−26 46 21.6	−11.87±0.11	+6.87±0.17
	35089	HD 56281	B8IV	...	07 15 23.88	−25 55 32.0	−1.7±0.4	+5.4±0.7
	35117	HD 56373	B9V	340±110	07 15 38.32	−26 51 24.3	−6.4±0.6	+4.4±1.1
	35166	HD 56472	B8–9IV	340±70	07 16 06.05	−26 49 23.0	+1.8±0.4	−3.1±0.7
	35326	HD 56876	B2IV/V	300±30	07 17 48.01	−26 47 51.2	−1.4±0.2	+0.9±0.3
	35421	CD–26 4162	B5	...	07 18 47.26	−26 57 06.7	−3.5±0.5	+2.7±0.9
	35611	HQ CMa AB	B2.5V+	800±200	07 20 54.92	−26 57 49.8	−5.0±0.2	+5.7±0.4
Escorial 16	34669	HD 54995	B4V	270±50	07 10 46.96	−09 20 09.6	−5.3±0.9	+3.2±0.6
	34680	HD 55013	A0	260±90	07 10 54.88	−09 27 07.6	−5.2±1.5	+4.7±1.1
	34707	HD 55117	B8V	(220±130)	07 11 16.98	−09 17 59.4	(−4.7±2.7)	(+3.1±2.0)
	34719	HD 55135	B4Vne	600±200	07 11 20.85	−10 25 43.8	−4.7±0.7	+3.0±0.5
	34818	HD 55419	B7V	500±200	07 12 26.35	−10 09 18.4	−6.5±1.1	+3.4±0.8
	34951	HD 55755	A0p	...	07 13 54.51	−10 13 16.7	−6.9±1.8	+3.8±1.3
	34953	HD 55754	B9V	210±40	07 13 56.15	−09 27 20.3	−0.8±1.0	−2.7±0.7
	34999	HD 55879	B0III	900±300	07 14 28.25	−10 18 58.5	−2.8±0.4	+1.4±0.3
	35050	HD 56007	B8V	...	07 14 54.57	−09 03 55.4	−2.6±1.4	+0.2±1.0
Escorial 17	34646	FF CMa AB	B4Vp+	...	07 10 30.63	−30 39 45.0	−1.3±0.9	+5.6±1.2
	34898	HO CMa AB	B5V+	600±300	07 13 13.07	−30 57 59.1	−3.4±0.5	+3.9±0.7
	34937	GG CMa	B2IV	430±70	07 13 47.23	−31 05 01.1	−5.2±0.3	+4.5±0.3
	34954	HD 55985	B2IV/V	530±90	07 13 57.34	−30 20 23.2	−4.5±0.2	+4.4±0.3
	34964	HD 56046	B6V	...	07 14 02.66	−31 38 33.4	−0.6±0.4	+3.7±0.5
	34968	HD 56045	B8V	440±180	07 14 08.61	−29 55 45.9	−3.2±0.6	+4.4±1.0
	35083	HD 56342	B3V	193±8	07 15 21.07	−30 41 11.2	−13.09±0.17	+11.98±0.19
	35168	MS CMa AB	B4V+	500±120	07 16 06.90	−30 26 07.3	−2.4±0.3	+3.8±0.4
	35342	HD 56998	B7III	260±40	07 18 02.66	−30 56 16.1	−2.9±0.4	+4.3±0.7
	35348	HD 56997	B9V	400±120	07 18 04.44	−30 27 11.7	+0.9±0.5	+1.2±0.7
	35391	HD 57120 AB	B3V+	...	07 18 33.41	−30 47 55.6	−2.2±0.8	+4.8±1.0
Escorial 18	35009	HD 56066	B8II/III	440±150	07 14 33.69	−24 56.16.5	−3.8±0.4	−0.2±0.6

Continued on next page.

Table A1: Continued.

Agglomerate	HIP	Name	Spectral type	d [pc]	α (J2000)	δ (J2000)	$\mu_\alpha \cos \delta$ [mas a^{-1}]	μ_δ [mas a^{-1}]
	35026	HD 56094	B2IV/V	510±140	07 14 42.10	−23 29 21.8	−3.8±0.3	+3.4±0.4
	35128	CD−24 5089	B5	...	07 15 43.54	−24 33 58.6	−2.2±0.9	+3.0±1.2
	35208	HD 56579	B3V	...	07 16 36.32	−23 49 36.7	−3.9±0.4	+3.2±0.5
	35267	HD 56694	B5V	430±140	07 17 10.27	−24 21 07.5	−2.3±0.5	+3.3±0.6
	35316	HD 56834	B8II	...	07 17 41.04	−23 10 59.0	−2.1±0.6	+4.6±0.7
	35329	HD 56848	B6III	600±300	07 17 49.41	−23 11 27.7	−4.6±0.6	+2.7±0.8
	35370	HD 56995	B2IV/V	...	07 18 21.94	−24 51 11.9	−3.2±0.6	+3.1±1.1
	35412	UW CMa AB	O7Iae+	580±90	07 18 40.38	−24 33 31.3	−2.21±0.18	+3.2±0.2
	35415	τ CMa AB	O7Ib+	...	07 18 42.49	−24 57 15.8	−2.3±0.4	+5.0±0.6
	35453	HD 57193	B1III	...	07 19 09.91	−25 33 57.2	−2.9±0.3	+3.4±0.5
	35461	MX CMa AB	B2V+	660±190	07 19 12.77	−24 57 20.5	−3.3±0.2	+4.0±0.4
	35503	HD 57281 AB	B5V+	[70±30]	07 19 37.50	−24 01 27.7	+10.2±3.0	+5.1±4.6
	35539	HD 57372 AB	Ap+	300±90	07 20 02.71	−24 24 57.5	−7.2±0.7	+2.0±1.0
	35597	CD−24 5234	B5V	290±130	07 20 46.27	−24 34 19.3	−1.3±1.0	+2.5±1.4
	35773	HD 58010	B2IV	...	07 22 45.18	−25 10 17.8	−1.6±0.5	+2.9±0.9
Escorial 19	35700	HD 57912	B9V	...	07 21 57.72	−32 11 28.0	−7.8±0.6	+4.4±0.8
	35761	HD 58063	B4V	500±100	07 22 35.65	−32 02 45.7	−8.0±0.3	+4.0±0.4
	35795	NO CMa	B5IIIne	410±40	07 23 00.70	−31 55 25.6	−7.53±0.17	+4.1±0.3
	35822	HD 58216	B8V	240±40	07 23 15.36	−32 02 48.1	−7.5±0.5	+3.8±0.6
	35855	HD 58286	B3III/IV	340±30	07 23 31.90	−32 12 07.4	−7.13±0.17	+4.4±0.2
	35859	HD 58285	B9III	380±80	07 23 34.65	−31 17 59.8	+2.1±0.4	−1.2±0.6
	35905	HD 58396	A0	...	07 24 07.10	−31 53 29.6	−9.0±1.0	+1.7±1.4
	36038	HD 58767 AB	B8−9V+	370±100	07 25 36.86	−32 30 33.3	−7.5±0.5	+3.5±0.7
	36045	HD 58766	B2V	340±40	07 25 42.98	−31 44 19.4	−7.8±0.3	+3.9±0.4
	36345	HD 59499 AB	B3V+	230±30	07 28 51.15	−31 50 54.2	−9.7±0.4	+3.7±0.6
Escorial 20	35996	HD 58563	B5III	290±130	07 25 07.08	−26 55 58.0	−4.1±0.8	+4.1±1.6
	36065	CD−26 4352	B9	(260±110)	07 25 55.54	−26 22 10.6	−4.8±0.9	−1.1±1.7
	36096	HD 58823	B2V	...	07 26 11.14	−26 14 10.0	−2.8±0.6	+3.9±1.2
	36222	HD 59138	B5III	...	07 27 33.98	−27 01 24.8	−3.8±0.6	+2.8±1.0
	36293	HD 59281 AB	B4Vne+	...	07 28 12.33	−27 23 58.8	−3.4±0.7	+3.4±0.8
	36323	HD 59364	B5V	(340±130)	07 28 36.53	−26 29 06.3	−9.8±0.7	+3.7±1.1
	36359	HD 59480	B8III/IV	(290±100)	07 29 03.14	−26 59 16.2	−4.1±0.7	+5.0±1.0
	36469	HD 59716	B9	...	07 30 14.87	−26 21 03.6	−3.0±0.7	+4.5±1.2
	36605	V375 Pup	B9III	...	07 31 40.58	−26 54 05.1	−4.9±0.5	+2.9±1.0
Escorial 21	36736	HD 60325	B2II	620±160	07 33 22.19	−14 20.17.9	−3.4±0.4	+0.6±0.3
	36967	HD 60856	B5V	600±300	07 35 56.96	−14 42 39.0	−6.7±0.7	+0.6±0.6
	36981	V378 Pup AB	B2−3Ve+	390±60	07 36 03.89	−14 29 34.0	−6.7±0.3	+0.4±0.3
	37015	HD 60969	B3III/IV	420±90	07 36 27.44	−14 35 42.3	−8.2±0.5	+1.2±0.4
	37037	HD 61017	B9III	410±80	07 36 41.25	−14 26 37.0	−5.7±0.4	+1.0±0.4
	37047	HD 61045	B7−8III	400±140	07 36 47.17	−14 33 41.8	−8.0±0.8	+0.9±0.6
Escorial 22	36944	HD 60879	B3V	...	07 35 41.46	−25 20 26.1	−5.2±0.4	+2.0±0.8
	36972	HD 60954	B3V	...	07 35 59.75	−25 30 42.7	−5.1±0.4	+3.6±0.9
	37006	HD 61025	B2Vne	410±140	07 36 18.12	−24 36 35.3	−2.0±0.7	+1.3±0.8
	37025	HD 61071 AB	B2III+	700±200	07 36 31.82	−25 19 58.0	−5.1±0.2	+4.0±0.4
	37173	m Pup A(C)B	B8IV++	190±9	07 38 18.05	−25 21 53.3	−3.03±0.13	−7.4±0.2
	37270	HD 61619	B8−9II	...	07 39 12.24	−25 26 43.2	−5.1±0.4	+2.9±0.8
Escorial 23	37215	HD 61512	Asp	250±30	07 38 33.71	−26 19 00.1	−3.3±0.2	+0.3±0.4
	37229	k^{01} Pup AB	B5IV+	110±8	07 38 49.87	−26 48 13.8	−16.8±0.3	+21.1±0.6
	37293	HD 61672	B7V	230±30	07 39 26.98	−26 51 47.2	−4.6±0.2	−4.2±0.3
	37304	HD 61687 AB	B6V+	193±18	07 39 29.85	−26 55 08.4	−5.5±0.2	−2.4±0.4
	37399	HD 61987	B4IV/V:	570±170	07 40 43.39	−27 56 43.3	−7.5±0.3	+5.3±0.4
	37482	HD 62191	B5III/IV	...	07 41 39.81	−27 13 59.2	−5.7±0.4	+5.0±0.5
	37544	HD 62312	B8III	290±60	07 42 19.25	−27 11 01.7	−3.7±0.4	+4.1±0.5
	37554	HD 62358	B8−9Ve	270±50	07 42 26.15	−27 43 47.6	−3.6±0.4	+0.0±0.5
Escorial 24	37297	HD 61831	B2.5V	170±5	07 39 27.34	−38 18 28.9	−21.11±0.14	+15.80±0.14
	37322	HD 61878 AB	B5Vn+	175±8	07 39 43.81	−38 08 21.4	−22.1±0.3	+16.5±0.2
	37329	HD 61899	B2.5V	350±30	07 39 47.88	−38 15 38.3	−10.40±0.19	+9.45±0.19
	37345	V468 Pup	B6IVe	430±40	07 39 57.99	−37 34 45.9	−0.84±0.18	−4.4±0.2
	37450	HD 62226	B5V	182±8	07 41 15.81	−38 32 00.7	−20.9±0.2	+16.3±0.2
	37514	HD 62376	B7V	181±14	07 41 58.03	−38 31 42.1	−17.3±0.4	+14.6±0.4
	37557	HD 62503	B9V	220±20	07 42 30.62	−39 12 04.5	−22.7±0.5	+15.6±0.6
	37666	HD 62712	B9Vsp	195±15	07 43 42.92	−38 12 06.8	−21.6±0.3	+15.7±0.5
	37697	HD 62803	B9V	160±13	07 44 02.50	−38 49 04.6	−22.8±0.4	+15.9±0.5
	37752	HD 62893	B7V	207±11	07 44 34.18	−37 56 34.5	−21.6±0.2	+15.6±0.3
	37803	HD 62991	B3IV	360±50	07 45 04.77	−37 53 16.3	−10.4±0.3	+5.0±0.4
	37838	HD 63079	B9V	204±17	07 45 27.36	−37 35 46.6	−22.9±0.3	+15.6±0.5
	37915	V392 Pup	B7V	181±8	07 46 10.54	−37 56 01.2	−19.6±0.2	+12.9±0.2
	38010	HD 63465	B2.5III	320±20	07 47 24.99	−38 30 40.1	−9.79±0.18	+5.1±0.2
Escorial 25	37765	HD 63007	B5V	270±20	07 44 40.22	−47 00 30.5	−13.1±0.3	+8.1±0.4
	37926	HD 63343	B5V	420±80	07 46 19.04	−46 09 34.7	−3.8±0.5	+8.4±0.5
	37953	HD 63449 AB	B7IV+	360±80	07 46 46.03	−46 48 06.0	−6.4±0.6	+7.3±0.8
	38020	HD 63578	B1.5IV	480±40	07 47 31.51	−46 36 30.6	−3.60±0.18	+8.55±0.19
	38028	HD 63579	B3V	500±90	07 47 35.21	−47 00 46.6	−4.0±0.4	+9.6±0.4
	38075	HD 63707	B6V	(500±200)	07 48 09.14	−47 16 32.3	−6.6±0.6	+11.6±0.6
	38159	QS Pup	B1.5IV	590±80	07 49 12.86	−46 51 27.8	−4.1±0.2	+9.9±0.2
	38164	P Pup AC	B0III	510±70	07 49 14.30	−46 22 23.5	−4.4±0.3	+8.6±0.3
	38294	HD 64248	B8V	520±170	07 50 45.79	−46 19 36.2	−4.6±0.7	+8.8±0.7
	38345	HD 64318	B3IV/V	490±70	07 51 13.97	−47 12.59.1	−3.2±0.3	+8.6±0.3
Escorial 26	39461	HD 67041	B3III/IV	...	08 03 56.04	−47 48 56.9	−1.2±0.4	+11.0±0.4

Continued on next page.

Table A1: Continued.

Agglomerate	HIP	Name	Spectral type	d [pc]	α (J2000)	δ (J2000)	$\mu_\alpha \cos\delta$ [mas a^{-1}]	μ_δ [mas a^{-1}]
	39576	HD 67314	B8V	420±90	08 05 12.98	−47 02 43.9	−6.3±0.6	+10.0±0.5
	39584	MX Vel	B3Vnp	1000±300	08 05 20.30	−46 58 42.3	−5.7±0.3	+6.9±0.3
	39679	HD 67612	B8–9V	410±90	08 06 32.39	−49 12 07.4	−10.4±0.6	+5.0±0.5
	39691	HD 67621	B2IV	390±40	08 06 41.61	−48 29 50.6	−5.4±0.2	+9.5±0.2
	39716	HD 67704	A0V	200±14	08 07 05.54	−47 47 37.8	−14.6±0.4	+19.3±0.4
	39717	HD 67705 AB	B8V+	500±130	08 07 05.67	−48 11 22.3	−6.2±0.5	+9.9±0.4
	39728	HD 67703	B9V	270±50	08 07 12.38	−46 38 27.0	−10.1±0.6	+10.1±0.6
	39768	HD 67820	B8IV	270±30	08 07 40.75	−47 15 17.6	−9.5±0.4	+7.2±0.5
	39773	HD 67847	B8V	223±15	08 07 41.78	−49 00 37.7	−16.8±0.4	+7.3±0.3
	39873	KW Vel	A0III	330±70	08 08 41.61	−49 29 50.0	−6.6±0.6	+7.7±0.6
	39919	NN Vel	B8Ib/II	300±20	08 09 09.51	−48 41 03.9	−9.1±0.3	−1.5±0.3
	39953	γ Vel A	O9IW+C8	330±40	08 09 31.95	−47 20 11.7	−6.2±0.3	+10.3±0.3
	39970	IS Vel	B2IV	340±20	08 09 43.15	−47 56 13.9	−5.91±0.19	+9.66±0.19
	39992	HD 68395	B4V	...	08 10 01.78	−47 49 05.9	−3.6±0.6	+6.4±0.5
	40011	HD 68451	B5II	330±50	08 10 16.08	−49 02 05.7	−8.7±0.5	+4.2±0.4
	40016	HD 68478	B3III/IV	540±80	08 10 20.56	−49 14 14.4	−9.7±0.3	+4.7±0.3
	40024	HD 68496	B6V	600±200	08 10 27.24	−49 09 50.9	−8.3±0.6	+4.2±0.6
	40059	HD 68608	B7III	440±120	08 10 59.55	−49 17 03.9	−9.3±0.6	+4.0±0.6
	40077	HD 68657	B3V	259±18	08 11 10.79	−48 27 43.2	−16.6±0.3	+4.5±0.2
	40336	HD 69282	B8V	600±300	08 14 08.89	−49 14 04.0	−9.8±0.6	+4.1±0.6
Escorial 27	40063	HD 68450	O9.5II	1000±300	08 11 01.68	−37 17 32.5	−4.5±0.3	+5.3±0.3
	40181	HD 68761	B0.5III	610±130	08 12 27.37	−36 59 21.2	−4.4±0.3	+5.7±0.3
	40218	HD 68843	B6Vnn	280±40	08 12 50.71	−36 13 41.3	−6.8±0.4	+7.2±0.4
	40255	HD 68944	B5V	300±40	08 13 18.19	−36 20 30.3	−6.3±0.4	+7.1±0.4
	40268	HD 68962	B2–3V	310±40	08 13 22.65	−36 18 37.5	−7.1±0.4	+7.2±0.4
	40274	MX Pup	B1.5IIIe	286±13	08 13 29.52	−35 53 58.3	−7.29±0.13	+9.76±0.15
	40321	OS Pup	B1.5IV	310±40	08 13 58.31	−36 19 20.2	−7.76±0.17	+7.81±0.19
	40324	HD 69082	B2IV/V	350±40	08 13 58.70	−36 20 26.8	−6.6±0.2	+7.8±0.3
	40328	HD 69106	B0.5II	480±110	08 14 03.80	−36 57 07.9	−4.6±0.4	+4.5±0.4
	40443	HD 69402	B4V	320±90	08 15 28.07	−37 22 19.3	−10.8±0.7	+4.8±0.8
	40519	HD 69620	B6V	270±30	08 16 24.99	−36 12 09.4	−10.0±0.3	+6.8±0.4
Escorial 28	40109	HD 68697	B7–8IV	380±70	08 11 33.64	−46 13 58.4	−7.3±0.6	+9.8±0.5
	40183	HD 68895 AB	B5V+	320±40	08 12 30.79	−46 15 51.4	−4.0±0.6	+9.1±0.3
	40285	NO Vel AB	B2.5IV+	420±40	08 13 36.15	−46 59 29.9	−10.1±0.2	+9.88±0.17
	40299	HD 69168	B2Ve	390±60	08 13 45.65	−46 34 43.3	−8.3±0.4	+3.8±0.3
	40357	HD 69302 AB	B2IV/V+	360±30	08 14 23.87	−45 50 04.3	−7.9±0.2	+10.6±0.2
	40397	HD 69404	B2Vnne	610±120	08 14 51.24	−46 29 09.2	−6.0±0.3	+7.6±0.6
Escorial 29	40586	HD 69934	B8–9V	600±200	08 17 12.56	−47 39 55.9	−8.4±0.6	+10.6±0.6
	40600	HD 69973	B4V	350±50	08 17 19.58	−47 55 12.3	−7.4±0.4	+10.0±0.4
	40662	IT Vel	B5II/III	420±70	08 18 01.15	−47 05 30.7	−9.1±0.4	+9.8±0.4
	40742	HD 70251	B8V	290±30	08 18 58.31	−47 12 39.4	−10.8±0.4	−1.8±0.4
	40749	HD 70309 A	B3III	250±50	08 19 05.58	−48 11 52.3	−14.2±0.4	+9.9±0.3
	40825	HD 70451	B7IV/V	900±400	08 19 57.92	−47 40 48.1	−13.5±0.5	+11.6±0.4
	40851	HD 70464	B9IIIp	700±300	08 20 08.12	−47 39 36.8	−11.4±0.6	+9.8±0.6
	40872	HD 70507	Ap	330±50	08 20 23.45	−46 59 32.1	−11.4±0.5	+8.1±0.5
	40921	HD 70643	B9IV	390±90	08 21 05.49	−46 59 57.5	−6.9±0.6	+9.1±0.4
	41013	HD 70851	B9IV/V	580±160	08 22 12.41	−47 46 57.7	−13.3±0.5	+14.7±0.4
Escorial 30	41737	HD 72350 AB	B4IV+	600±200	08 30 39.23	−44 44 14.4	−10.0±0.5	+4.3±0.4
	42007	HD 72919	B8–9V	700±300	08 33 42.60	−44 56 45.8	−6.4±0.6	+7.7±0.6
	42036	HD 72997	B2II/III	580±150	08 34 08.14	−44 32 41.4	−6.2±0.4	+6.6±0.4
	42041	HD 73010	B5V	700±200	08 34 11.12	−45 38 11.7	−11.5±0.5	+6.9±0.5
	42073	HD 73059	B7II/III	...	08 34 30.02	−44 30 22.6	−7.6±0.9	+5.1±0.8
	42085	HD 73090	B5II/III	...	08 34 40.59	−44 31 41.9	−6.0±0.6	+5.9±0.5
Escorial 31	42400	HD 73952 AB	B8Vn+	161±9	08 38 44.81	−53 05 25.4	−25.5±0.4	+21.9±0.3
	42459	HD 74071	B5V	137±4	08 39 23.84	−53 26 23.2	−23.8±0.2	+23.5±0.2
	42504	NZ Vel	B4IV	136±6	08 39 57.60	−53 03 17.0	−25.3±0.4	+22.1±0.4
	42535	HD 74196	B7Vn	147±6	08 40 17.46	−53 00 55.4	−25.4±0.3	+23.2±0.2
	42536	o Vel	B3IV	152±8	08 40 17.59	−52 55 18.8	−24.4±0.4	+34.4±0.3
	42715	KT Vel AB	B8s+	154±6	08 42 18.99	−53 06 00.2	−23.6±0.3	+24.2±0.3
	42726	HY Vel	B3IV	149±4	08 42 25.39	−53 06 50.3	−24.83±0.18	+23.22±0.18
Escorial 32	42595	HD 74234	B2IV	700±200	08 40 53.40	−48 13 31.8	−4.5±0.4	+2.8±0.4
	42605	HD 74251	B3IV/V	(700±300)	08 41 01.57	−48 04 02.9	−8.7±0.5	+8.2±0.5
	42614	HD 74273	B1.5V	610±80	08 41 05.32	−48 55 21.6	−4.3±0.2	+3.8±0.2
	42698	HD 74436 AB	B3V+	...	08 42 07.5	−48 14 40.8	−5.1±0.7	+4.6±0.8
	42712	HX Vel AB	B1.5Vn+	(520±150)	08 42 16.19	−48 05 56.7	−4.4±0.3	+3.4±0.3
	42738	HD 74531 A	B2V:	...	08 42 34.84	−48 09 48.9	−3.5±0.4	+3.0±0.4
Escorial 33	43055	HD 75083	B7–8V	390±120	08 46 17.68	−42 45 31.2	−11.1±0.7	+6.7±0.7
	43085	HD 75126 AB	B3III/IV+	350±60	08 46 33.10	−42 33 58.6	−11.6±0.5	+6.0±0.4
	43182	HD 75324	B4V	330±70	08 47 47.93	−42 16 22.3	−12.8±0.4	+6.0±0.4
	43209	HD 75387	B2IV/V	490±70	08 48 08.76	−42 27 48.4	−12.4±0.3	+6.3±0.2
	43240	HD 75446	B6V	350±60	08 48 30.83	−42 24 02.4	−12.9±0.4	+6.0±0.4
	43303	HD 75608	B6V	340±80	08 49 21.26	−43 22 14.4	−8.3±0.4	+4.6±0.4
	43326	CD–42 4684s AB	A8+	400±80	08 49 40.27	−42 49 24.5	−12.7±0.6	+6.6±0.5
	43346	HD 75655	B2III	770±150	08 49 47.48	−41 44 35.4	−5.5±0.4	+4.5±0.4
	43392	HD 75759 AB	B1.5III+	580±180	08 50 21.02	−42 05 23.2	−5.3±0.2	+3.2±0.2
	43450	HD 75850	B8–9V	370±60	08 51 00.06	−41 56 49.4	−13.4±0.5	+6.5±0.6
Escorial 34	100518	HD 194206	B8V	900±300	20 22 57.65	+39 12 39.7	+2.4±0.2	−0.4±0.3
	100603	HD 194424	B8IV	...	20 24 02.81	+39 32 29.4	+1.2±0.5	−1.7±0.5
	100644	HD 194480	A2	...	20 24 26.00	+38 57 54.1	+2.4±0.4	−0.9±0.5

Continued on next page.

Table A1: Continued.

Agglomerate	HIP	Name	Spectral type	d [pc]	α (J2000)	δ (J2000)	$\mu_\alpha \cos\delta$ [mas a^{-1}]	μ_δ [mas a^{-1}]
	100702	HD 194576	B8III	(600±300)	20 24 58.79	+39 50 21.7	+2.0±0.6	−2.8±0.6
	100741	HD 194670	B8V	370±70	20 25 28.58	+39 47 36.7	+5.8±0.4	+1.4±0.4
	100784	HD 194789	B8	330±40	20 26 03.86	+40 24 06.2	+7.2±0.3	+3.0±0.3
	100833	HD 194908	B9	300±40	20 26 43.77	+40 20 50.0	+6.4±0.4	+0.4±0.4
	100834	HD 194885	A0	260±20	20 26 43.77	+39 29 45.3	+4.1±0.3	+2.4±0.3
Escorial 35	111337	HD 213801 AB	B9V+	410±180	22 33 23.47	+39 34 30.6	−2.2±1.2	−5.2±1.1
	111400	HD 213918 AB	Ap+	...	22 34 07.28	+39 20 07.9	+0.7±1.1	−8.8±0.9
	111544	8 Lac B	B2V	...	22 35 52.09	+39 37 41.3	...	...
	111546	8 Lac A	B2Ve	...	22 35 52.29	+39 38 03.6	+0.1±1.5	−5.2±1.3
	111576	HD 214243	B6IV	360±100	22 36 16.67	+40 05 19.6	−0.1±0.9	−2.8±0.7
	111683	HD 214432	B3V	580±170	22 37 28.72	+39 26 19.9	−1.7±0.6	−4.6±0.4